

Birth events, masses and the maximum mass of Compact Stars

Jorge E. Horvath^{1,*}, Lívia S. Rocha¹, Antônio L. C. Bernardo¹, Marcio G. B. de Avellar², Rodolfo Valentim²

¹Universidade de São Paulo, Instituto de Astronomia, Geofísica e Ciências Atmosféricas, Rua do Matão 1226, 05508-090, São Paulo - SP, Brazil

²Instituto de Ciências Ambientais, Químicas e Farmacêuticas (ICAQF), Departamento de Física, Universidade Federal de São Paulo - UNIFESP, Rua São Nicolau no.210, Centro, 09913-030, Diadema - SP, Brazil

*E-mail: foton@iag.usp.br

Half-title page, prepared by publisher

Publishers' page

Full title page, prepared by publisher

Copyright page, prepared by publisher

Contents

Birth events, masses and the maximum mass of Compact Stars

Jorge E. Horvath^{1,}, Livia S. Rocha¹, Antônio L. C. Bernardo¹, Marcio G. B. de Avellar², Rodolfo Valentim²*

1.	Birth events, masses and the maximum mass of Compact Stars	1
1.1	Introduction	1
1.2	The sample of neutron stars and its mass distribution . .	2
1.2.1	Types of mass measurements	2
1.2.2	Exploring the mass distribution of neutron stars .	5
1.3	Maximum mass of (non-rotating, isotropic) neutron stars .	12
1.3.1	TOV equations for relativistic stellar structure . .	14
1.3.2	The Rhoades-Ruffini limit of a neutron star mass	15
1.3.3	Redback/Black Widows binary systems and the maximum mass/lightest black hole problem . . .	22
1.3.4	GW detection events and the possibility of NS masses above $\sim 2.5 M_{\odot}$	25
1.4	Gravitational waves from merging NS	26
1.4.1	Inferring the masses of NS from GW events	27
1.4.2	Asymmetry in the systems GW170817 and GW190425	30
1.5	Neutron star birth events	32
1.5.1	Neutron stars formed in single explosions	32
1.5.2	Neutron stars formed in binaries	38
1.5.3	The Accretion-Induced Collapse channel for NS formation	39

1.6	Conclusions	41
	<i>Bibliography</i>	43

Chapter 1

Birth events, masses and the maximum mass of Compact Stars

1.1 Introduction

At the beginning of the current century a scientific magazine published an article mentioning 11 unanswered questions of Physics whose resolutions could provide a new era in science (Haseltine, 2002). Among them is the behaviour of matter at ultrahigh densities and temperatures, a challenging topic that is directly related with neutron stars (NSs) Physics.

Such extreme conditions make it impossible to deal with this type of matter in a laboratory, therefore the equation of state (EoS) governing these compact objects cannot be attained by experimental methods only. This is the reason why is so important to direct efforts to the observational, theoretical and computational fields of NSs, in order to extract their bulk properties, reveal how matter behaves in their interior and how related phenomena are generated, such as supernovae explosions. For example, in the observational realm, macroscopic parameters like mass and radius are tightly related with microphysics inside the star and can help to set reliable constraints on it.

Neutron stars are the densest and smallest stars observed in the Universe, with a mean density of $\langle \rho \rangle$ exceeding the ordinary nuclear density $\rho_{sat} = 2.8 \times 10^{14} \text{ g/cm}^3$. Such an extreme density corresponds to a baryon number density of $n_{sat} \sim 0.16 \text{ fm}^{-3}$. There is evidence that these stars are the final stage of the life of ordinary stars whose masses are in the range $\sim 9.0 M_{\odot} < M < 25.0 M_{\odot}$ (Heger *et al.*, 2003) (although this is far from established, see Section 1.5) or even an outcome of an Accretion Induced Collapse of a white dwarf (or a pair of them, see below) (Ruiter *et al.*, 2019). Neutron stars are considered “dead” because they have stopped producing nuclear energy as remnants of the stellar evolution of massive

stars. They can be observed in various astrophysical sources, from radio to X-ray pulsars, X-ray bursters, compact thermal X-ray sources in supernovae remnants and in binary systems (some of them relativistic), among many possibilities.

As a consequence of their compactness, neutron stars must be described in terms of General Relativity, thus the introduction of an appropriate EoS in the Einstein Field Equations and its hydrostatic equilibrium consequence, the Tolman-Oppenheimer-Volkoff (TOV) equation, leads to the existence of a maximum value for the mass of the star (see Sec. 1.3). The observation of very massive NSs in the last decade had profound implications for the open question mentioned above, because it establishes a lower limit on the maximum mass, and thus helps to set realistic constraints for matter beyond nuclear saturation density ρ_{sat} ruling out models that do not support masses in the observed range, and also helps to classify an object as a Black-Hole (BH) if its mass is above the maximum allowed value for NSs. All these issues will be briefly reviewed here to gain insight on the state-of-the-art of this problem and suggest future directions.

1.2 The sample of neutron stars and its mass distribution

From the first observation of a pulsar in 1967 by Jocelyn Bell (Hewish *et al.*, 1968) until now, computational and instrumental developments, especially in the current century, helped to increase the available sample of objects and improved precision on measurements with new generations of high-quality telescopes. In particular, the masses of the NSs has been targeted to connect them with the birth events and the properties of superdense matter. We present now an overview of these issues.

1.2.1 Types of mass measurements

The vast majority of NSs are observed as pulsars, rapidly-rotating and high-magnetized neutron stars emitting beams of radiation along its magnetic axis that are seen on Earth as a pulse due to the lighthouse effect (Rezzolla *et al.*, 2018b). Nowadays, more than 2800 pulsars were observed (see <https://www.atnf.csiro.au/research/pulsar/psrcat/> for a catalogue of radio pulsars), but only a few aspects of them can be inferred from observations and only a tiny fraction of the total sample allows mass measurements because observed pulsars are mainly isolated stars and the calculation methods are generally based on orbital motions, although efforts

are beginning to be made to measure features of isolated NSs (Horvath, 1996).

The extreme regularity of pulses, responsible for recognizing pulsars as the most stable clocks in the observable universe, makes *pulsar timing* the most accurate method to determine masses of NSs, as well as test fundamental physics. The procedure consists in monitoring the times-of-arrival (TOAs) of pulses over several years to determine the pulsar's rotation period. Thanks to the regularity, small deviations of TOAs are detectable with precision. Additional parameters of pulsar and its orbit (in binary systems) are also obtained from pulsar timing.

Orbital motion of binary systems is described by five Keplerian parameters: binary period P_b , projection of pulsar's semimajor axis (a_p) on the line of sight $x_p = a_p \sin i$, eccentricity e , time T_0 and longitude ω of periastron. The masses of components can be determined from a mass function in light of Kepler's Third Law:

$$f_1(m_1, m_2, i) = \frac{(m_2 \sin i)^3}{(m_1 + m_2)^2} = \frac{4\pi^2 x_p^3}{T_\odot P_b^2}, \quad (1.1)$$

where $T_\odot \equiv GM_\odot/c^3 = 4.925490947 \mu s$ (G is the gravitational constant, c is the speed of light and M_\odot is the solar mass) (see Chap. 9 of Shapiro and Teukolsky (2008) for a pedagogical discussion of the mass function).

Whenever mass functions are measurable, it is possible to obtain individual masses provided the inclination angle i is known, but this quantity is difficult to be inferred with accuracy and the mass function of the companion is only obtained in some cases where it is a detectable pulsar or a star with an observable spectrum. However, binary systems containing a pulsar are compact and thus some relativistic effects might be observed. The relativistic corrections for orbital motion for GR are described in terms of post-Keplerian (PK) parameters, which are functions of Keplerian parameters (Stairs, 2003):

(i) Orbital period decay, \dot{P}_b :

$$\dot{P}_b = -\frac{192\pi}{5} \left(\frac{P_b}{2\pi T_\odot} \right)^{-\frac{5}{3}} \left(1 + \frac{73}{24}e^2 + \frac{37}{96}e^4 \right) (1 - e^2)^{-\frac{7}{2}} \frac{m_p m_c}{m^{1/3}}; \quad (1.2)$$

(ii) Range of Shapiro delay, r :

$$r = T_\odot m_c; \quad (1.3)$$

(iii) Shape of Shapiro delay, s :

$$s = \sin i = x_p \left(\frac{P_b}{2\pi} \right)^{-2/3} \frac{m^{2/3}}{T_\odot^{1/3} m_c}; \quad (1.4)$$

(iv) "Einstein delay", γ :

$$\gamma = e \left(\frac{P_b}{2\pi} \right)^{1/3} T_\odot^{2/3} \frac{m_c (m_p + 2m_c)}{m^{4/3}}; \quad (1.5)$$

(v) Advance of periastron, $\dot{\omega}$:

$$\dot{\omega} = 3 \left(\frac{P_b}{2\pi} \right)^{-5/3} (1 - e^2)^{-1} (m T_\odot)^{2/3}. \quad (1.6)$$

In Eq. (1.2)-Eq. (1.6) the subindexes of Eq. (1.1) were changed from 1 to p standing for the pulsar component and from 2 to c for the companion, and $m = m_p + m_c$. If only one PK parameter is observed, constraints can be imposed on individual masses. The observation of any two PK parameters allows unique individual mass determinations, and if extra parameters are specified it is possible to test GR (Lyne *et al.*, 2004).

Millisecond pulsars (MSPs) are pulsars with very short spin periods, $1 < P < 30$ ms and $\dot{P} < 10^{-19}$, which were spun-up by its companion during a transfer of angular momentum to the NS, being *recycled*. These short periods make MSPs extremely precise for pulsar timing and they are now recognized as the most useful objects to test fundamental physics (Özel and Freire, 2016).

For a large number of binaries only one PK parameter is measured, but as mentioned before in cases where the companion is optically observed (main sequence, post-main sequence and white dwarfs stars) it is possible to provide additional information about the system. Phase-resolved spectroscopy provides orbital radial velocity amplitude (K_c), which together with Keplerian parameters yields the mass ratio ($q = m_p/m_c$). For white dwarfs, particularly, their radii can be estimated if the distance to Earth is known and the optical flux and effective temperature are measured. Thus, from a theoretical relation based on their spectrum its mass can be obtained, leading to the pulsars mass estimation through the relation of mass ratio. For NSs with high-mass companions, x-rays emitted by the pulsar are blocked by the companion during part of its orbit, allowing mass measurements also.

The Shapiro delay, in its turn, consists in an retardation of pulses TOA due to space-time curvature near a massive companion. This effect can

remain unobserved, even after years of timing, if it is too small, but for almost edge-on MSP systems containing a high-mass WD, the effect is strong enough and allows extremely precise measurements of both masses. PSR J1614-2230 with $1.97 \pm 0.04 M_{\odot}$ (Demorest *et al.*, 2010) (latter corrected for $1.928 \pm 0.017 M_{\odot}$ by (Fonseca *et al.*, 2016)) and PSR J0740+6620 with $2.14^{+0.10}_{-0.09} M_{\odot}$ (Cromartie *et al.*, 2020) are two MSPs that became important references when talking about imposing a lower limit for the maximum mass of NSs where measured through Shapiro delay. However, there is more overall information in the whole distribution that can be exploited, even if the individual measurements are not that precise. We turn to this question in the rest of this Section.

1.2.2 *Exploring the mass distribution of neutron stars*

Although pioneers works pointed for the possibility of a wide range of masses for neutron stars, the old idea of a unique-mass scale with a small dispersion around a central value was strengthened by the theoretical argument on the pre-supernova explosion, in which an iron core supported by electron degeneracy (thus with an almost invariant mass) gives place to a NS with a slightly lower mass. Observational works seemed to converge with the theoretical statement for decades. Finn (1994) employed for the first time a statistical analysis of a sample of four double neutron star systems (DNS) with the constrained masses of eight NS and found that masses should fall predominantly in the range $1.3 < m/M_{\odot} < 1.6$. Thorsett and Chakrabarty (1999) obtained a mean value of $1.35 \pm 0.04 M_{\odot}$ for a sample of 19 NS masses, and no evidence for a significant dispersion around the single scale.

The rapid development of instrumental and computational fields, specially at the turn of the century, prompted a paradigm questioning and break. New observations put on stage old arguments about a different supernova mechanism leading to the formation of lighter pulsars. On the other hand, X-ray and optical observations provided evidence for the existence of masses above $2 M_{\odot}$, despite large uncertainties, bringing up accretion histories and/or NSs that are born massive. As seen in van den Heuvel (2004), a speculation of the possible existence of three neutron star classes already existed. The current sample of NS mass measurements and its uncertainties is shown in Fig. 1.1, with different types of binary systems distinguished by colors.

Technological advances has provided us with faster and higher-capacity

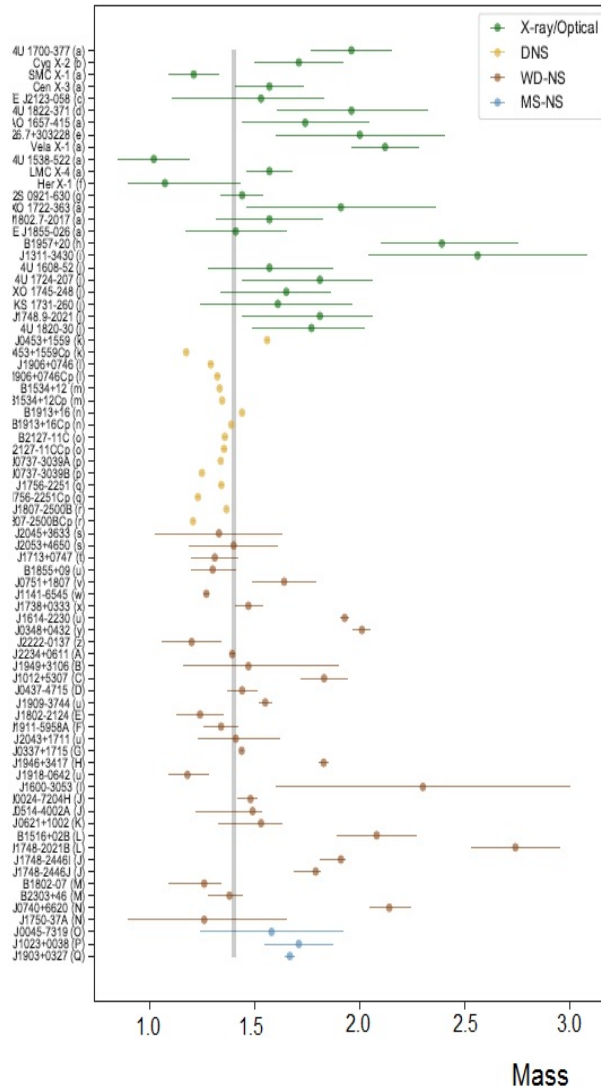


Fig. 1.1: Masses compiled by L.S. Rocha as October/2020. a)Falanga *et al.* (2015), b)Casares *et al.* (2010), c)Tomsick *et al.* (2004), d)Munoz-Darias *et al.* (2005), e)Bhalerao (2012), f)Rawls *et al.* (2011), g)Steehgs and Jonker (2007), h)Van Kerkwijk *et al.* (2011), i)Romani *et al.* (2012), j)Özel *et al.* (2016), k)Martinez *et al.* (2015), l)Van Leeuwen *et al.* (2015), m)Fonseca *et al.* (2014), n)Weisberg *et al.* (2010), o)Jacoby *et al.* (2006), p)Kramer *et al.* (2006), q)Ferdman *et al.* (2014), r)Lynch *et al.* (2012), s)Berezina *et al.* (2017), t)Zhu *et al.* (2015), u)Fonseca *et al.* (2016), v)Desvignes *et al.* (2016), x)Antoniadis *et al.* (2012), w)Bhat *et al.* (2008), y)Antoniadis *et al.* (2013), z)Kaplan *et al.* (2014), A)Stovall *et al.* (2019), B)Deneva *et al.* (2012), C)Antoniadis *et al.* (2016), D)Reardon *et al.* (2016), E)Ferdman *et al.* (2010), F)Bassa *et al.* (2006), G)Ransom *et al.* (2014) H)Barr *et al.* (2017), I)Arzoumanian *et al.* (2018), J)Kiziltan *et al.* (2013), K)Kasian (2012), L)Freire *et al.* (2008), M)Thorsett and Chakrabarty (1999), N)Cromartie *et al.* (2020), O)Nice (2003) , P)Deller *et al.* (2012), Q)Freire *et al.* (2011)

computers, permitting the Bayesian approach to spread among scientific community through *Markov Chain Monte Carlo* (MCMC) simulations. Bayesian analyses became an allied for Astronomy, embracing also the study of NS physics, including the formation channels and evolution histories, especially because it is quite suitable for small samples. Several works employed these techniques to extract information from the mass distribution (Valentim *et al.*, 2011; Zhang *et al.*, 2011; Özel *et al.*, 2012; Kiziltan *et al.*, 2013; Antoniadis *et al.*, 2016; Farrow *et al.*, 2019; Linares, 2019), each of them choosing their own *prior* models particularity. For example, Schwab *et al.* (2010), discussed the evidence of a bimodal distribution based on a sample of 14 masses, where a peak in $\sim 1.25 M_{\odot}$ might be related with electron-capture supernovae (Nomoto, 1984; Podsiadlowski *et al.*, 2004) and a peak in $\sim 1.35 M_{\odot}$ related with the Fe core-collapse supernovae. This e-capture SN is supposed to occur in a very degenerate O-Ne-Mg core in progenitors, quenching the development of an iron core, being triggered by a sudden capture of electrons onto Ne nuclei when a critical mass is reached (see Sec. 1.5).

Generally speaking, the mass distribution of observed NS masses (the likelihood in the Bayesian language) can be modeled as a Gaussian mixture with n components:

$$\mathcal{L}(m_p|\theta) = \sum_i^n r_i \mathcal{N}(m_p|\mu_i, \sigma_i), \quad (1.7)$$

where μ_i and σ_i are the mean and standard deviation of i -th normal component \mathcal{N} and r_i is its relative weight, satisfying $\sum_i^n r_i = 1$ to ensure normalization.

Frequentist inferences for the mass distribution Although Bayesian statistics have gained strength over the years, frequentist non-parametric hypothesis tests are also commonly employed by astronomers (about 500 refereed papers each year in astronomical literature), to help exploring tentative conclusions about different phenomena and to better understand the data. Kolmogorov-Smirnov (K-S) and Anderson-Darling (A-D) are two well-known suitable examples of hypothesis tests.

Both tests are based on the maximum distance between *empirical distribution function* (EDF) of the sample and the *cumulative distribution function* (CDF) of a specified distribution. The K-S statistic is most sensitive to large-scale differences in location and shape, whilst A-D statistic is sensitive for both large and small-scale differences and also weights the tails of

distributions, presenting a more robust result (Babu and Feigelson, 2006). A p-value is extracted from tests and the model is rejected or not related to a significance level α . By default $\alpha = 0.05$, so the hypothesis is rejected if $p < 0.05$. We applied both K-S and A-D tests for the sample of NSs shown in Fig. 1.1 to compare unimodal, bimodal and trimodal distribution models. For the model with one Gaussian we set $\mu = 1.48$ and $\sigma = 0.35$, while for the 2-component model $\mu_i = \{1.38, 1.84\}$, $\sigma_i = \{0.15, 0.35\}$ and $r_i = \{0.6, 0.4\}$, with $i = \{1, 2\}$ respectively. Lastly, for the 3-component model we assume $\mu_i = \{1.25, 1.40, 1.89\}$, $\sigma_i = \{0.09, 0.14, 0.30\}$ and $r_i = \{0.10, 0.5, 0.4\}$ for $i = 1, 2, 3$. Resultant p-values are shown in Table 1.1. The simplest (unimodal) model is ruled out in both K-S and A-D tests. Both 2 and 3-component models are not rejected, and presents a similar p-value. Figure 1.2 shows in the panel (a) the EDF of sample in black, and the CDF of three mentioned models used for tests calculations, showing that unimodal distribution (blue) fits well the position of mean but is bad in adjusting tails while the bimodal (red) and trimodal (green) curve provide better fits along all the sample distribution. Panel (b) shows the PDF of all models together with the sample histogram. As stated above, hypothesis tests help to gather a intuitive comprehension of the problem, but are sensitive to the parameter values and are not conclusive.

Table 1.1: P-value of two hypothesis test for three different models

Model	K-S	A-D	Conclusion
Unimodal	0.025	0.032	Reject
Bimodal	0.971	0.990	Do not reject
Trimodal	0.974	0.953	Do not reject

Bayesian Approach Bayesian statistics is based on *Bayes theorem* derived from axioms on conditional probabilities. In the case one is interested in the probability distribution of a parameter θ (or a set of parameters) that describes a model, based on observed data (D), the posterior distribution of it is set as:

$$P(\theta|D) = \frac{\mathcal{L}(D|\theta)P(\theta)}{P(D)}, \quad (1.8)$$

where $P(\theta)$ is called *prior distribution* and represents previous information about the model and $\mathcal{L}(D|\theta)$ is the *likelihood function* which describes the

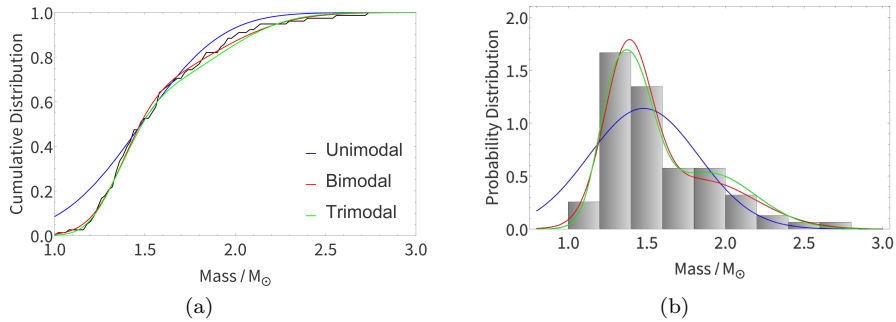


Fig. 1.2: (a) The black curve represents the EDF of sample, while the blue curve is the CDF of an unimodal distribution, the red curve is the CDF of a bimodal distribution and in green is the CDF of a trimodal distribution. As can be noted the blue curve provides a good fit to the mean position, but is quite bad in adjusting the tails. (b) The histogram of observed masses is shown, together with PDF of the 3 mixture models. Although the p-value of 2 and 3-component models are similar, the three peaks of the last one are not clearly identified, even if the binning is reduced.

distribution of observed data, conditioned by the parameters. Depending on the adopted family distribution and on the dimension of parameter space, the main difficulty of calculating posterior distributions is in the normalization term $P(D) = \int P(\theta)P(D|\theta)d\theta$. MCMC methods provide an efficient way for sampling a given distribution, bypassing the problem of accounting for $P(D)$. We recommend Sharma (2017) and references therein for those who want to familiarize with MCMC algorithms. An extensive list of algorithms to perform MCMC sampling is available today, so the better choice for a given problem will depend on the specific purposes to be attained.

The features and shape of the distribution obtained from sampling methods helps to better comprehend the formation and evolution of NSs in different systems. The old model of a single-mass scale around $1.35\text{--}1.4 M_{\odot}$ is expressed as unimodal, so $n = 1$ in order to represent a unique mood for NS formation. However, today is known that $m_p \geq 2.0 M_{\odot}$ exist, therefore the mass distribution needs to be at least bimodal ($n = 2$) to accommodate these heavy objects, with the lower peak accounting for stars formed from the “normal” Fe core-collapse supernova and the higher peak ones may contain “directly formed” NSs, AIC remnants and NSs with a substantial accretion history. In order to analyze the existence of a different supernova mechanism forming (electron-capture) lighter NSs, as mentioned before, an

extra component must be introduced in the model ($n \geq 3$).

Model comparison to determine which one is favorable respect to data can be done by many different techniques, depending on aspects of the model and chosen algorithm. Two of the most famous techniques are the Bayesian Information Criterion (BIC) and the Akaike Information Criterion (AIC), although some statisticians do not recommend them. Both methods are based on the calculation of posterior likelihood, penalizing the model due to the number of parameters and sample size (for BIC).

We have performed a Bayesian analysis to the sample shown in Fig. 1.1, assuming that the maximum mass allowed for NSs m_{\max} to be located at 3σ to the right of the highest-value peak (referring to heavier objects). As we are dealing with Gaussian distributions, values within three standard deviations (to the left and right) account for 99,73% of the distribution, so there is a very small probability of finding a NS with a mass higher than that.

The unimodal model, were all objects are assumed to belong to the same distribution peak with a likelihood given by:

$$\mathcal{L}(m_p|\theta) = \mathcal{N}(m_p|\mu, \sigma), \quad (1.9)$$

results unlikely, in agreement with previous works mentioned here and the frequentist result shown before.

Bimodal model results are the favored one in our analysis. The likelihood of this model is:

$$\mathcal{L}(m_p|\mu_i, \sigma_i, r_i) = r_1\mathcal{N}(m_p|\mu_1, \sigma_1) + r_2\mathcal{N}(m_p|\mu_2, \sigma_2). \quad (1.10)$$

The prior distributions were assumed as a $Beta(2,2)$ for the relative weights, $r = \{r_1, r_2\}$, a Gaussian $\mathcal{N}(0, 2)$ for $\sigma = \{\sigma_1, \sigma_2\}$, and a Gaussian $\mathcal{N}(1.45, 0.30)$ to $\mu = \{\mu_1, \mu_2\}$.

When trying to account for the peak of NSs formed by the electron-capture supernovae, in addition to the “common” ones and the accretion history leading to heavy objects, with a likelihood:

$$\begin{aligned} \mathcal{L}(m_p|\mu_i, \sigma_i, r_i) = & r_1\mathcal{N}(m_p|\mu_1, \sigma_1) + r_2\mathcal{N}(m_p|\mu_2, \sigma_2) \\ & + r_3\mathcal{N}(m_p|\mu_3, \sigma_3), \end{aligned} \quad (1.11)$$

we found that we could not distinguish the peak around $1.25 M_{\odot}$. Despite the fact that the progenitors of these objects are expected to be abundant in the Universe (as mentioned in Sec. 1.5), this result can be interpreted as if only a tiny fraction of observed neutron stars arise from these events (although the reason would be unknown), but it is not unlikely that improved statistical schemes can separate this peak.

In Bayesian analysis parameters are random variables, and not fixed values as in frequentist analysis, so they are expressed in terms of marginalized posterior distributions, which we summarized in Table 1.2. The mean value for each parameter is in the second column, followed by the corresponding standard deviation in the third column. Fourth and fifth columns presents the Highest Posterior Density from which we conclude that, for example, $1.305 < \mu_1 < 1.398$ with a 94% credible interval.

Table 1.2: Parameter estimation of bimodal model trough MCMC methods in the Bayesian framework. The second column shows the mean value of each parameter, followed by the corresponding standard deviation. Fourth and fifth columns present the highest posterior density.

Parameters	mean	sd	HPD (3%)	HPD (97%)
r_1	0.588	0.105	0.382	0.775
r_2	0.412	0.105	0.225	0.618
μ_1	1.351	0.025	1.305	1.398
μ_2	1.756	0.098	1.581	1.944
σ_1	0.087	0.023	0.047	0.133
σ_2	0.286	0.069	0.154	0.414

Although in this case m_{\max} is a generated quantity and not a free parameter of the model, it depends on the values of μ_2 and σ_2 so it is also a random variable given by a distribution shown in Fig. 1.3. As a summary we have $m_{\max} = 2.616 \pm 0.196$ for the mean and standard deviation, with a 94% credible interval in $\{2.273, 2.985\}$, a skewed distribution. This will be of relevance to understand the meaning of several high masses (and particularly the lighter one of the event GW190408) as we will be seen below.

Recently, Alsing *et al.* (2018) also presented a Bayesian analysis (for a sample of 74 NSs) using Gaussian mixtures models with $n = \{1, \dots, 4\}$ components and an additional investigation on m_{\max} . For each n two routines were implemented, one where the maximum mass is fixed at $m_{\max} = 2.9 M_{\odot}$, and other where it is set as a free parameter bounded by $m_{\max} < 2.9 M_{\odot}$. They found that $n = 2$ and $m_{\max} < 2.9 M_{\odot}$ were favored among all models. The posterior result also shows a sharp cut-off on maximum mass distribution, with a peak in $2.12 M_{\odot}$ as shown in Figure 3 of their work that shows the marginalized posterior distribution of the

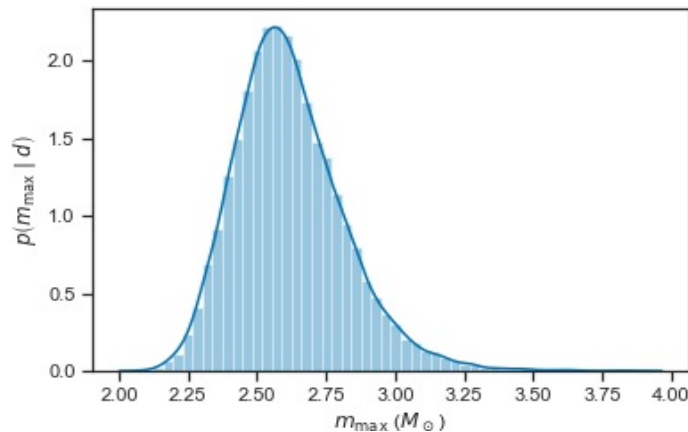


Fig. 1.3: Maximum mass distribution in the case where it is assumed to be located at $3\sigma_2$ to the right of μ_2 .

maximum mass, with a 90% credible interval in $2.0 < m_{\max} < 2.6 M_{\odot}$. Although the distribution reaches values $\sim 2.6 M_{\odot}$, they have a low probability, so this result is disfavoured when considering a scenario in which heavy NSs are expected to exist.

We have conducted our own calculations leaving M_{\max} as a free parameter to be determined (and penalized) by the Bayesian algorithm with the result given in Fig. 1.3. Even though there is a wide distribution of possible M_{\max} the peak is precisely around the same value $M \sim 2.5 M_{\odot}$, giving support to the idea that the “light” component of GW190408 may be a NS near the TOV limit. Studies along these lines are guaranteed to establish this important issue.

1.3 Maximum mass of (non-rotating, isotropic) neutron stars

As final states of massive star evolution (and possibly additional formation channels as well), NSs are relativistic objects and as such, the pressure term becomes important for their structure as a source of gravity. Theory predicts the existence of a maximum mass for neutron stars resulting from the Tolman-Oppenheimer-Volkoff equation, the General Relativistic version of the hydrostatic equilibrium discussed in Sec. 1.3.1. The exact value of

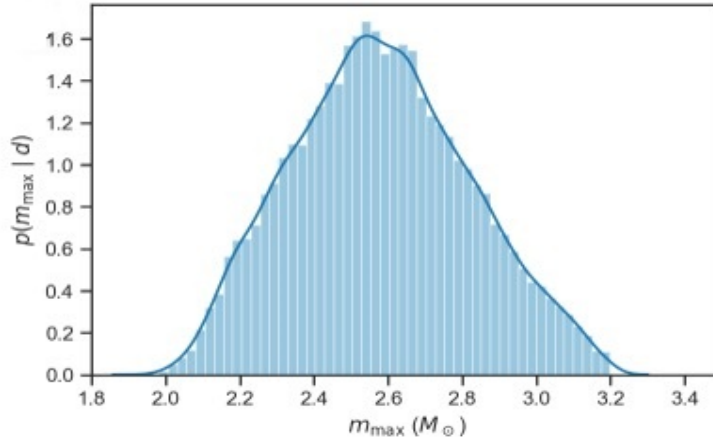


Fig. 1.4: Maximum mass distribution as determined from the sample of Fig. 1.1 as a truncation of the second Gaussian peak centered at μ_2 .

m_{TOV} depends on the EoS, in any case, but the EoS itself is difficult to pin down and remains uncertain. Many of the EoS reflect mostly different compositions, from pure neutrons to baryon rich matter to even exotic matter composed by a soup of u , d and s asymptotically free quarks (Özel and Freire, 2016; Lattimer, 2012; Heiselberg and Pandharipande, 2000). The EoS of dense matter, i.e., the relation between pressure and (energy) density, is informative of the composition and the inner structure of a NS (Glendinning, 2012; Weber, 2017; Özel and Freire, 2016). Observational parameters like the mass or the radius have an intrinsic correlation with the EoS, albeit a complex one.

Irrespective of any experimental data, Rhoades Jr and Ruffini (1974) derived a theoretical limit of $3.2 M_{\odot}$ for the maximum mass of any compact object independent of the exact nature of the EoS. This is a result based on general relativistic arguments, together with Le Chatelier's principle. We discuss this limit in Sec. 1.3.2. Today, we know that the Rhoades and Ruffini limit is *not* an absolute mass limit in the general situation (for example, anisotropic models can violate the Rhoades-Ruffini limit), but it is still considered a milestone of the knowledge of the dividing line between neutron stars and black holes. As mentioned before, the observation of a very massive neutron star poses stringent constraints on the EoS of these objects, and also sets the lower limit for black holes masses.

1.3.1 Tolman-Oppenheimer-Volkoff equations for relativistic stellar structure

Oppenheimer and Volkoff (1939), based on the previous work on spherically symmetric metrics in GR by Tolman (1934), published a seminal paper where they derived the relativistic equations for hydrostatic equilibrium. This equation taken together with the continuity of the mass, written below, completely determine the structure of spherically symmetric, static neutron stars:

$$\frac{dP}{dr} = -\frac{G\rho m}{r^2} \left(1 + \frac{P}{\rho c^2}\right) \left(1 + \frac{4\pi Pr^3}{mc^2}\right) \left(1 - \frac{2Gm}{rc^2}\right)^{-1}, \quad (1.12)$$

where $m(r)$ is defined by:

$$\frac{dm}{dr} = 4\pi r^2 \rho. \quad (1.13)$$

Solving the TOV equations for a compact star implies integrating the equations, usually from the center ($r = 0$) to the surface ($r = R$) where the pressure vanishes, with the aid of an equation of state, i.e., a function relating pressure and density. Besides, for solving the TOVs is necessary two boundary conditions: $m(0) = 0$ and $\rho(0) = \rho_c$. However, this procedure implies some assumptions throughout the calculations; inside the star, we must have (Chamel *et al.*, 2013):

- (1) $\rho \geq 0$: the mass density should be positive;
- (2) $dP/d\rho \geq 0$: the NS matter must remain in an equilibrium state (Le Chatelier's principle);
- (3) $P \geq 0$: the pressure should be positive;
- (4) $dP/dr \leq c^2$: the sound speed should not exceed c

Conditions 1-4 imply that the pressure decreases from the center to the star's surface, guaranteeing the integration of the TOVs given a value for the central pressure through the EoS. A general characteristic of these equations is that they naturally produce a maximum mass for the compact star. This feature is a purely general relativistic effect due to the denominator factor $(1 - 2Gm/rc^2)$ of the pressure gradient, and the presence of the pressure added to the energy density in the numerator of Eq. (1.12).

The nature of the resulting objects depends upon the exact properties of the equation of state. Oppenheimer and Volkoff, for example, used an equation of state for degenerate Fermi gas of neutrons, obtaining a maximum mass of only $0.7 M_\odot$.

At the time of these writings the catalog of neutron star measured masses fills almost one hundred entries, and their distribution points to masses ranging from 1.1 to $2.7 M_{\odot}$ as shown in Fig. 1.1. The higher mass confidently detected is $m = 2.14_{-0.09}^{+0.10} M_{\odot}$ for the millisecond pulsar MSP J0740+6620 (Cromartie *et al.*, 2020).

Theoretically, we learned a lot about the properties of matter at high and supranuclear densities, and now we know that equations of state must allow masses above $2.14M_{\odot}$, and that other measurements and arguments may push this limit above $2.5M_{\odot}$, surprisingly closer to the original Rhoades-Ruffini value to be addressed below.

1.3.2 The Rhoades-Ruffini limit of a neutron star mass

Establishing the maximum mass of neutron stars is vital not only to understand the true nature of matter inside it but also to set the limit from where the formation of a black hole is unavoidable. As stated above, the exact nature of matter at supranuclear densities is a long-posed problem for which a solution is still nowadays elusive, this is why the availability of an “absolute” value for the limit mass is so important.

In fact, as Rhoades Jr and Ruffini argued in 1974, it is not really necessary to know the exact equation of state to obtain a valid theoretical limit. This theoretical limit on the mass comes from well-established physical principles that all the matter should obey, which are:

- (1) The compact star must obey the General Relativistic equation for hydrostatic equilibrium;
- (2) Matter must obey the Le Chatelier Principle, stating that a disturbance in a system in equilibrium will be opposed to restoring the equilibrium;
- (3) Matter must obey the Principle of Causality, which implies that the sound speed must remain lower than the speed of light in the medium.

To comply with these three requirements, Rhoades Jr and Ruffini assumed that the EoS is uncertain above a fiducial density of $\rho_{\star} = 4.6 \times 10^{14} \text{ g/cm}^3$, the region in which they assumed that the equation of state is the stiffest possible, producing a sound velocity equal to the velocity of light. Thus, they found a maximum possible mass for a neutron star of about $3.2 M_{\odot}$.

The Rhoades-Ruffini mass limit can be expressed as (see Chamel *et al.*, 2013):

$$m_{RR} \simeq 3.0 \left(\frac{5 \times 10^{14}}{\rho_\star} \right)^{1/2} [M_\odot]. \quad (1.14)$$

As a conclusion, all compact objects whose mass is measured to be higher than $3.2 M_\odot$ must be a black holes provided it is non-rotating, isotropic and GR holds.

As a further development, allowing the violation of the causality, using an incompressible fluid, the mass limit can be expressed as (see Chamel *et al.*, 2013):

$$m_{RR,non-causal} \simeq 5.09 \left(\frac{5 \times 10^{14}}{\rho_\star} \right)^{1/2} [M_\odot]. \quad (1.15)$$

In Eq. (1.14) and Eq. (1.15), ρ_\star is the value assumed to be the fiducial one.

It is worth stressing again that the Rhoades-Ruffini limit does not take into account other effects that, as we will see below, allows matter inside the NS to support masses higher than $3.2 M_\odot$. Examples of these effects are rotation and anisotropies in the fluid's pressure, discussed in Sec. 1.3.2.1.

1.3.2.1 *Types of neutron star models*

The several decades of work showed that, although the Rhoades-Ruffini limit meaning remains strictly unchallenged, realistic equations of state hardly achieve the limit of causality. However, quite recently actual data is “pushing” the actual maximum mass towards the Rhoades-Ruffini extreme.

On the one hand, the maximum mass exact value is determined by the equation of state. The better knowledge we now have about the behavior of matter above supranuclear densities allows us to infer different compositions for the inner core of neutrons stars, and each one produces a unique value for the maximum mass.

A NS is usually depicted as an onion-like object whose structure is something like: a fragile gaseous plasma atmosphere \sim centimeters thick; a \sim few-meter deep liquid plasma “ocean”; a few hundred meters thick atomic *outer crust* followed by a 1-2 kilometers crystal lattice of neutrons and protons immersed in an electron gas and neutron-rich liquid *inner crust*. All these layers altogether, however, add up from 0.01 to 0.1 of the star's total mass, and their composition is relatively well-known from nuclear physics (Haensel *et al.*, 2007; Chamel *et al.*, 2013).

The equation of state of the crust up to densities of $\sim 2\rho_{\text{sat}}$ (where $\rho_{\text{sat}} = 2.8 \times 10^{14} \text{ g/cm}^3$ is the nuclear saturation density) is relatively well-known, and common equations of state used in calculations include the Baym-Pethick-Sutherland (Baym *et al.*, 1971) equation of state and the HP (Haensel and Pichon, 1993).

Things begin to get complicate at the core of the star, divided into two regions: the outer core, with densities ranging from $\rho_{\text{sat}}/2$ to $2\rho_{\text{sat}}$, and the inner core with densities ranging from $2\rho_{\text{sat}}$ to around $10\rho_{\text{sat}}$ (Haensel *et al.*, 2007; Chamel *et al.*, 2013). Neutrons (mostly), protons, electrons, and muons compose the neutron star's outer core. The composition of the inner core is, actually, the long-posed mystery about NSs. The inner core is also the dominant structure for the neutron star's mass budget. Depending on the approach to the behavior of matter at densities higher than $\sim 5 \times 10^{14} \text{ g/cm}^3$, in the inner core region, one builds a sequence of stars with a unique value of the maximum mass.

Figure 1.5 shows examples of several sequences of stars, each built by a specific EoS. Each EoS produces a unique value of maximum mass. In this figure we also show, represented by the magenta horizontal stripes, some observed values for the mass of the most massive neutron stars ever detected, and a candidate to the uttermost massive neutron star: PSR J1614-2230 ($m = 1.928 \pm 0.016 M_{\odot}$ (Fonseca *et al.*, 2016)), PSR J0740+6620 ($m = 2.14_{-0.09}^{+0.10} M_{\odot}$ (Cromartie *et al.*, 2020)), and the compact object in GW190814 ($m = 2.59_{-0.09}^{+0.08} M_{\odot}$, (Abbott *et al.*, 2020c)).

That said, there are “types” of equations of state to describe the inner core (see (Chamel *et al.*, 2013)). The first of these types is the hadronic one, where matter is assumed as a liquid of nucleons only, i.e., protons and neutrons, the whole structure being neutralized by a lepton gas such electrons and, at very high densities, muons. This nuclear matter has been studied since the '50s, as the many approaches in many-body calculations were becoming available. Also, heavy-ion experiments are used to gauge the models, making the EoS more realistic. Some representatives of this family are the following equations: AP 1 (Akmal and Pandharipande, 1997), ENG (Engvik *et al.*, 1994), MPA 1 (Müther *et al.*, 1987), MS 1 (Müller and Serot, 1996), SLY (Douchin and Haensel, 2001), and WFF 1 (Douchin and Haensel, 2001).

Although such calculations produce similar results up to $5 \times 10^{14} \text{ g/cm}^3$, as the density becomes high the predictions open a fan of different results, producing maximum masses from 1.8 to $2.5 M_{\odot}$, the first case revealing that the EoS are too soft for supporting recent determinations of neutron

Mass-radius relation for several EoS

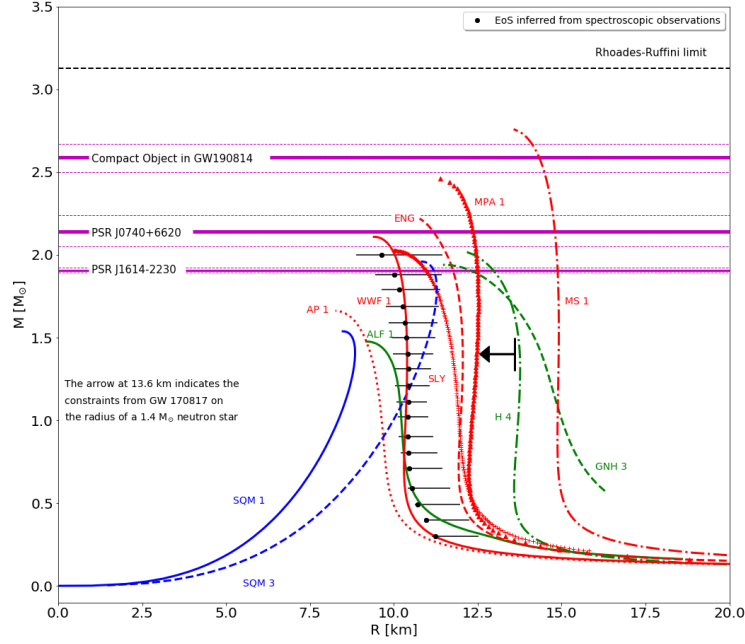


Fig. 1.5: Mass-radius relation for several equations of state, named in the Figure, illustrating the “families” of equations of state. The hadronic EoS are the AP 1, ENG, MS 1, MPA 1, SLY and WWF1; the hybrid ones are the ALF 1, GNH 3 and H4; the ones with strange quark matter are the SQM 1 and SQM 3. The black dots represent an EoS inferred from spectroscopic observations. The data for this $M - R$ diagram and the observational dots were taken from <http://xtreme.as.arizona.edu/NeutronStars/> (Earlier compilations and naming conventions are from Lattimer and Prakash 2001 and Read et al. 2009. The full list included above is from (Özel and Freire, 2016)) In this Figure, we also plot: PSR J1614-2230 ($m = 1.928 \pm 0.016 M_{\odot}$), PSR J0740+6620 ($m = 2.14^{+0.10}_{-0.09} M_{\odot}$), and the compact object in GW190814 ($m = 2.59^{+0.08}_{-0.09} M_{\odot}$). The sequences were calculated from the TOV, i.e., they do not include rotation.

star masses.

In a sense, the recent detection of the very massive millisecond pulsars, or the successive LIGO-VIRGO reports of the GW170817 coalescence of two compact objects into an object with $\geq 2.4 M_{\odot}$ rule out soft hadronic EoS. On the theoretical side, it has been known that the possible appearance of kaon and pion condensates at high densities implies that the equation of state should be even softer, and some exotic mechanisms have been suggested to circumvent this softening to match the observations. Some kind of repulsion must be introduced to match high masses, otherwise the sequences fall short to produce room for $\geq 2M_{\odot}$ stars.

The second type of model comes from the formation of *hyperons* or another species that will populate the core of the star at the high-density inner core. Brueckner-Hartree-Fock (BHF) calculations using realistic two- and three-body forces suggest to be unavoidable the appearance of hyperons, and this makes the EoS containing them extremely soft, producing a maximum mass of at most $1.4 M_{\odot}$. This situation has been called the *Hyperon Puzzle*. However, it is still possible to circumvent the hyperon puzzle at densities above $\sim 5 \times 10^{14} \text{ g/cm}^3$ with the relativistic mean-field calculation approach by “tuning” hyperonic coupling interactions. Some representatives of this family are the following EoS: ALF 1 (Alford *et al.*, 2005), GNH 3 (Glendenning, 1985), and H4 (Lackey *et al.*, 2006).

A third type comes with the deconfinement of nucleons into quarks. By this, we mean a soup of u and d quarks in asymptotic freedom that can produce neutron stars with masses in agreement with observations. However, this agreement is only achievable if the EoS for the quark matter has a stiffness so that the sound velocity is close to the velocity of light (however, never achieving the Rhoades-Ruffini mass limit discussed before). If quarks appear at high density, at some critical density, we may have quark cores for the so-called “hybrid models”.

However, there is an extreme version of this deconfinement scenario, the *strange star* picture. This hypothesis of the *absolute stability* of a quark matter with strangeness originated in 1971 with Bodmer and his speculation that the true ground state of matter was not the one we know from ordinary physics. Then, Witten (1984) calculated that this ground state would be a mixture of u , d and s quarks attained at supranuclear densities $\rho \sim 10^{15} \text{ g/cm}^3$.

If deconfinement is achieved in compact objects, then neutron stars would be almost certainly “strange stars” (so named because of the almost equal proportion between the upper, down, and strange quarks). Strange

stars show significant differences with normal neutrons stars: to begin with, the absence of an onion-like structure. Another critical difference is that the surface density is as huge as $\sim 10^{15} g/cm^3$, which is not that different from the center's density. It is not that difficult to produce maximum masses larger than $2 M_{\odot}$ (Horvath, 2007), around the values recently observed, provided the interactions represented in the vacuum energy and/or related quantities have suitable values, contrary to the earliest views about the softness of a relativistic quasi-massless gas of quarks (see, for instance, Franzon *et al.* (2012)).

Some representatives of the third type, strange stars, are the following EoSs: SQM 1 and SQM 3 (Prakash *et al.*, 1995). See also Bodmer (1971), Witten (1984) and Alcock *et al.* (1986). A complete survey of SQM EoS previous to pairing and other issues is given in Benvenuto and Horvath (1989).

In the end, the quest for the exact equation of state of neutron stars is still far from being closed, but recent observations and measurements of neutron stars masses seem to push the theory to stiff EoS. To view the heat of the debate, Shibata *et al.* (2019) constrained the maximum mass of a neutron star to less than $2.3 M_{\odot}$ using the detection of the event GW 170817. Soon after the paper of Wu *et al.* (2020) showed that neutron stars could have masses greater than $2.3 M_{\odot}$ if the equation of state could become stiffer in some regime. To study the stiffness of the EoS, the authors employed polytropic models dependent upon two free parameters in two scenarios, with a similar spirit than the Rhoades-Ruffini approach. For hadronic neutron stars, there would be a transition density above which the stiffening occurs. In this case, the transition would occur at $\rho_t/\rho_{\text{sat}} = 0.5$ if the polytropic index is $\gamma = 2.65$. In the scenario of strange stars, the compact object would support $m > 2.3 M_{\odot}$ if the two free parameters are in the range $(\rho_s/\rho_{\text{sat}}; \gamma) = (1.0 - 1.58; 1.40 - 2.0)$, where ρ_s is the surface density of these self-bound systems.

Still, using polytropic EoS, O'Boyle *et al.* (2020) presented a generalized piecewise polytropic parametrization for neutron star equations of state. The innovation of their method was to impose, despite the continuity in pressure and energy density, the continuity in the sound speed in the fluid. This generalized parametrization has advantages over the old one in hydrodynamic simulations of neutron star mergers since the tidal deformability is sensitive to the sound speed c_s , which is discontinuous in old approaches. The tidal deformability, in turn, strongly influences the gravitational waves produced at merger events.

Application of the generalized piecewise polytropic parametrization goes in the sense of recover the correct EoS parameters from observables in a secure way, providing strong constraints on the maximum mass of neutron stars, shedding light on the fundamental physics of black holes formation and the nature of dense matter.

Anisotropies in the stellar fluid are also an exciting approach for calculating the stellar structure and have been widely used to include a new degree of freedom, especially when dealing with exact solutions of the Einstein Field Equations (Sharma and Maharaj, 2007; de Avellar and Horvath, 2010; Rocha *et al.*, 2020). The extra degree of freedom allows one to impose an analytical EoS, as the MIT Bag Model, and an *ansatz* for a functional form of the metric elements.

Anisotropies inside compact stars can be significant for high densities, e.g., $\geq 10^{15}$ (Ruderman, 1972). One consequence is that they allow a higher central density, which augments the pressure support against gravitational collapse, leading the star to higher masses. Using the simple MIT Bag Model (Witten, 1984; Alcock *et al.*, 1986) and Sharma *ansatz* (Sharma and Maharaj, 2007), de Avellar and Horvath (2010) reached a maximum mass compatible with the observations of PSR J0740+6460. Rocha *et al.* (2020), on the other hand, reached maximum masses ranging from 3 to 5 M_{\odot} using the Thirukkanesh-Ragel-Malaver *ansatz* (Thirukkanesh and Ragel, 2012; Malaver, 2014) and an exact form for a CFL-type EoS (Rajagopal and Wilczek, 2001; Lugones and Horvath, 2002, 2003; Alford *et al.*, 2005).

On the other hand, studies on (quasi-)universal relations (involving, for example, the moment of inertia or the quadrupole moment, among others, known as “I-Love-Q”), and the role of rotation allow for making new and improved predictions, i.e., place new constraints almost independently of the equation of state.

Recently Breu and Rezzolla (2016) derived, from universal relations, that uniform rotation would increase the maximum mass up to 20% for all the equations of state they considered: they found $m_{\max} = (1.203 \pm 0.022) m_{\text{TOV}}$, where m_{TOV} is the maximum mass from solving the non-rotating TOV equations. Applying this result on the maximum mass resulting from some EoS, one can get a value compatible with recent observations such as GW190814.

Finally, we point out that compact objects are also studied within so-called *braneworld* models with extra dimensions (Lugones and Arbañil, 2017). By solving the stellar structure equation in the braneworld and using two types of EoSs (a hadronic one and a strange quark matter one),

the authors found that a new branch of stellar configurations arises for masses above 2 in which the causal limit can be violated. Not only this implies that there is no maximum mass in a braneworld neutron star but also that these very massive stars are stable against (small) radial perturbations, being supported by non-local effects of the bulk on the brane.

Thus, as we see from Fig. 1.5, although some equations of state can support masses compatible with recent observations, the detection of the compact object in GW190814, whose mass is $\sim 2.5 M_{\odot}$, poses a new challenge to the theory of dense matter provided it is indeed a NS. Not even rotation would allow a straightforward match. Is the compact object in GW190814 the lower limit for a black hole?

The general conclusion of this discussion is that there is no “absolute” in the Rhoades-Ruffini maximum mass limit (see, for example, Fig. 1.6). It can be violated in some circumstances, and the maximum mass could be higher than $3.2M_{\odot}$ within these models.

1.3.3 *Redback/Black Widows binary systems and the maximum mass/lightest black hole problem*

As explained in the Sec. 1.2, from the first determinations to the beginning of the 21st century, the idea that neutron star masses cluster around $1.4 M_{\odot}$, called the “canonical mass”, was settled in favor of a wider distribution. As newer accurate data from double neutron star systems and other binaries became available, it was revealed that neutron stars with masses as high as $2.14 M_{\odot}$ exist, suggesting that, at the very least, another higher mass scale should be considered.

“Spider” systems - black widows and redbacks, - are a class of relativistic binary systems in which the neutron star strongly interacts with its ordinary companion stars (Fruchter *et al.*, 1988; Roberts, 2012; Hui and Li, 2019). This interaction is possibly different from what we see in other binary systems, such as low-mass X-ray binaries, since two new ingredients come into play: the back illumination onto the donor and the ablation of the donor by the pulsar wind in the later stages.

The evolutionary history of these systems suggests a connection between redbacks and black widows through accretion, going back until the formation of the neutron star itself (Benvenuto *et al.*, 2012, 2014). The systems at formation time should have initial orbital periods of about one day. On a nuclear timescale of the secondary, the accretion sets in, but at a highly variable rate, due to a variety of effects. The authors in Benvenuto *et al.*

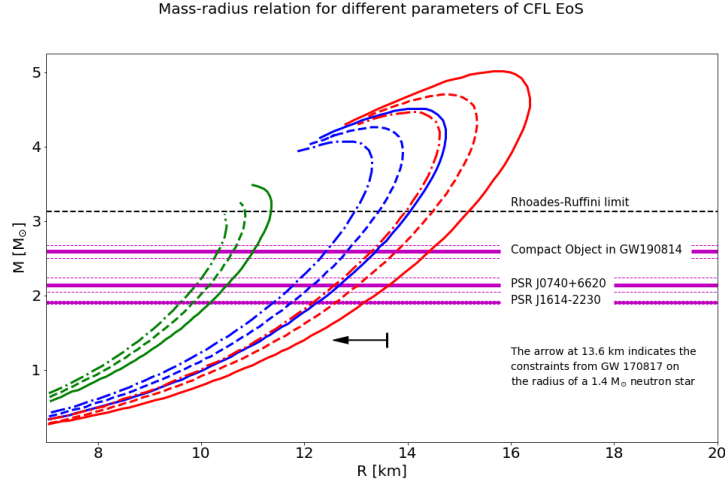


Fig. 1.6: Mass-radius relation for different parameters of the CFL equation of state, using Thirukkanesh-Ragel-Malaver *ansatz* for the metric element $e^{-2\lambda(r)}$. For solid lines, we assume $\Delta = 100 \text{ MeV}$ and $m_s = 150 \text{ MeV}$, while for the dashed lines, we assume $\Delta = m_s = 0 \text{ MeV}$ (resembling the MIT bag model), and for the dash-dotted lines $\Delta = 150 \text{ MeV}$ and $m_s = 150 \text{ MeV}$. Also, for the red lines we set $B = 57.5 \text{ MeV}/\text{fm}^3$, for the blue lines $B = 70 \text{ MeV}/\text{fm}^3$, and for the green lines $B = 115 \text{ MeV}/\text{fm}^3$. Figure adapted from Rocha *et al.* (2020).

(2012) present a complete model calculation of this scenario, showing the oscillations in the rate of accretion due to the so-called *quasi-Roche Lobe overflow* state.

A critical observation for the scenario mentioned above, of relevance to our discussion here, is that it takes a long time until the donor star enters the degenerate regime, allowing the neutron star to accrete a substantial fraction of a solar mass. Therefore, if the efficiency of the accretion is not too low, the scenario may produce very massive neutron stars. In Fig. 1.7 we show the measured masses of 17 redbacks/black widow systems.

Because of this feature, we may expect that the spider systems can shed light on the value of the maximum mass of neutron stars, as soon as new observations become available. If, contrary to widespread beliefs, nature produces very massive objects they will be a challenge to the physics of dense matter and to the actual mass difference between the m_{max} and the

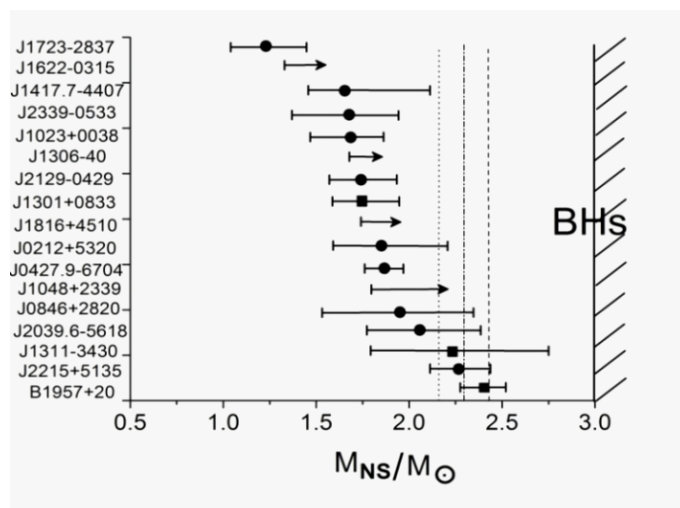


Fig. 1.7: The masses of Redback/Black Widows NSs. The circles denote a Redback system and the squares a Black Widow one. Lower limits on the masses of J1622-0315, J1306-40, J1816+4510 and J1048+2339 are indicated with the arrows. The dotted vertical line is the maximum mass derived by Margalit and Metzger (2017), the dashed-dotted line the upper limit of the range quoted by Ruiz *et al.* (2018) and the dashed line the value of Ai *et al.* (2020) for the SMNS formation case in the GW170817 merger. It is apparent that the lower numbers begin to collide with direct observations unless significant systematic errors are present. Other inferences are available and do better in this sense (see Table 1.3), allowing higher maximum masses. (full data of the direct observations and references can be found in Özel and Freire (2016) and Linares (2019)). The hatched region on the right marks the region of BHs, although strictly speaking all object pushed above will be BHs before the vertical line. Figure from Horvath *et al.* (2020)

Rhoades-Ruffini limit itself. Several NSs in spiders shown in Fig. 1.7 have been reported to be above the $2M_{\odot}$ mark.

Within this evolutionary scenario, Redback/Black Widows NSs may harbor the highest masses in nature, and can be an alternative channel to form low-mass BHs by pushing some NS masses over the TOV limit. This new channel is not subject to the constraints of gravitational collapse involved in the existence of the mass gap between high-mass NSs and low-mass BHs. However, the number of low-mass BHs formed in spider systems

must be small due to the restrictive conditions, as suggested by (Benvenuto *et al.*, 2012, 2014). The detection strategy must rely on the existence of accretion in binary systems where a compact object is present and the orbital periods are of the order of 1 day or less. Of course, typical requisites of redback and black-widow donors must also be fulfilled. An interesting candidate has been studied by Tetarenko *et al.* (2016). The binary system VLA J2130+12 is at a distance of $2.2_{-0.3}^{+0.5}$ kpc. Its compact object is a stellar black hole whose mass is *assumed* to be $10 M_{\odot}$ in the analysis. Other features of this system are a $0.1 - 0.2 M_{\odot}$ companion star and an orbital period of about 1-2 hours. We suggest that it may be still possible to identify the compact object with a black hole with a smaller mass descendant of NS pushed over the TOV limit if one does not assume anything about the mass *a priori*.

There are other methods to detect the existence of low-mass BHs other than by the spider channel. For instance, the LIGO event detection S200316bj was reported to have a probability of 0.9957 in favor of a black hole with $3 - 5 M_{\odot}$ (see LIGO/VIRGO Candidate Database available at <https://gracedb.ligo.org/superevents/S200316bj/view/>). Other channels cannot be discarded yet, and new methods such the eLISA, when it becomes operational, will improve our knowledge of the many channels, finally exploring the actual structure of the mass gap between neutron stars and black holes.

1.3.4 *GW detection events and the possibility of NS masses above $\sim 2.5 M_{\odot}$*

The gravitational wave detection events have opened a window of opportunity for studying the physics of dense matter. Initially, the LIGO/VIRGO experiments detected gravitational waves from a BH merger, one with $\sim 36 M_{\odot}$ and other with $\sim 29 M_{\odot}$ resulting in a BH with $\sim 62 M_{\odot}$.

The first detected NS-NS merger event was GW170817, with individual masses between $1.17 - 1.60 M_{\odot}$ and with a total mass of $2.74_{-0.01}^{+0.04} M_{\odot}$ (see some references in Table 1.3). GW170817 was the first GW event confirmed by non-gravitational counterparts, proving that it was the result of the collision of two neutron stars.

Later works on GW170817 inferred values for the maximum mass of the resulting neutron star, using different assumptions. As we see in Table 1.3, the mass inferences are dangerously close to the Rhoades-Ruffini mass limit, revealing that not only the equation of state of neutron stars must be stiff,

but also that other effects can be at play, like rotation and anisotropies.

Table 1.3: Inferred value of M_{TOV} from the behavior of GW170817 according to a) Shao *et al.* (2020); b) Ai *et al.* (2020); c) Shibata *et al.* (2019); d) Ruiz *et al.* (2018) ; e) Rezzolla *et al.* (2018a); f) Margalit and Metzger (2017) ; g) Alsing *et al.* (2018)

Value [M_{\odot}]	Type of the resulting object/assumption
$2.13 \pm_{0.07}^{0.08}$ (a)	SMNS
$2.09 \pm_{0.09}^{0.11}$ (b)	SMNS
$2.43 \pm_{0.08}^{0.10}$ (b)	SMNS
$2.43 \pm_{0.08}^{0.10}$ (b)	SNS
2.3 (c)	Conserv. + simulation
2.16 – 2.28 (d)	Minimal assumption
$2.16 \pm_{0.15}^{0.17}$ (e)	–
2.17 (f)	–
2.6 (g)	(3σ)

One final remark is motivated by the recent release of a complete analysis of the GW population (Abbott *et al.*, 2020b), which found a “gap” between the lightest GW190408 component at $\sim 2.6M_{\odot}$ and the second lightest object with $\sim 6M_{\odot}$, surely a black hole. If true this analysis reinforces the idea of a “mass gap”, but also suggests that the controversial $\sim 2.6M_{\odot}$ should be a NS. When the number of GW mergers increases in the next years this “gap” will be explored thoroughly. This is a clear example of the interplay between GW measurements and local NS Astrophysics previously stated.

In the end, it seems likely that the solution for the long-standing quest for the correct equation of state of neutron stars and, consequently, for the maximum mass of these unusual compact objects, will be settled by Gravitational Wave Astronomy, explored in Sec. 1.4.

1.4 Gravitational waves from merging NS

The discovery of the system PSR B1913+16 Hulse and Taylor in 1974 exposed the first detected pulsar in a binary system around another neutron star. The system has its orbit shrinking in precise agreement with Ein-

stein's General Theory of Relativity. The shrinkage of the orbit is due to the emission of Gravitational Waves (GW). This was the first indirect measurement of GW, granting Hulse and Taylor the Nobel Prize of Physics in 1993 for that contribution.

Gravitational Waves are perturbations on spacetime curvature, resulting from accelerated masses that propagate at the speed of light outwards from the source, decaying with the inverse of the distance. After decades of technological developments and tests, the first *direct* detection of GW was made in 2015 by the LIGO/VIRGO collaboration (Abbott *et al.*, 2016b,a), although since the 1960s attempts were made using resonant mass antennas, large masses of metal that would oscillate with the passage of GWs. Detections using this method were claimed, but never validated or consensual.

The new generation of GW detectors are very large (4 km) interferometers of high precision that are able to observe relative changes in length as small as 10^{-21} cm. The active ones are the two interferometers from the LIGO and VIRGO collaboration. These observatories are placed in a way that allow the triangulation of the event with a fairly reasonable precision (usually around 20 deg^2) and in conjunction with the wave analysis is possible to estimate the distance and the so-called chirp mass of the system \mathcal{M} for the case of merging objects.

The chirp mass is an observable quantity that can be expressed as $\mathcal{M} = M [q/(1+q)^2]^{3/5}$ where q is the quotient of masses and M the total mass of the merging system. Note that it is not possible to determine both masses independently without further assumptions as e.g. the distribution of masses or spin of the objects.

1.4.1 *Inferring the masses of NS from GW events*

The determination of the chirp mass \mathcal{M} is straightforward and very precise, being obtained from the GW frequency evolution as the objects coalesce. The main source of uncertainty is the redshift from the event to the geocentric frame, but still less than 1%. In contrast, the mass quotient q is degenerate with the alignment of the spins with the orbital angular momentum, imposing a dependency between the two quantities.

Another way to approach the problem of individual masses determination is to use the distribution of *observed* NS masses. It is generally assumed that merging NSs have a higher probability to have their masses within the most populated places of the diagram of masses (Valentim *et al.*, 2011).

For example, for $\mathcal{M} = 1.18M_{\odot}$ it is more plausible to have two NSs around $1.36M_{\odot}$, since it is in the most populated region of the diagram, than one with (say) $2M_{\odot}$ and the other with $1M_{\odot}$ where no NSs in DNSs are found.

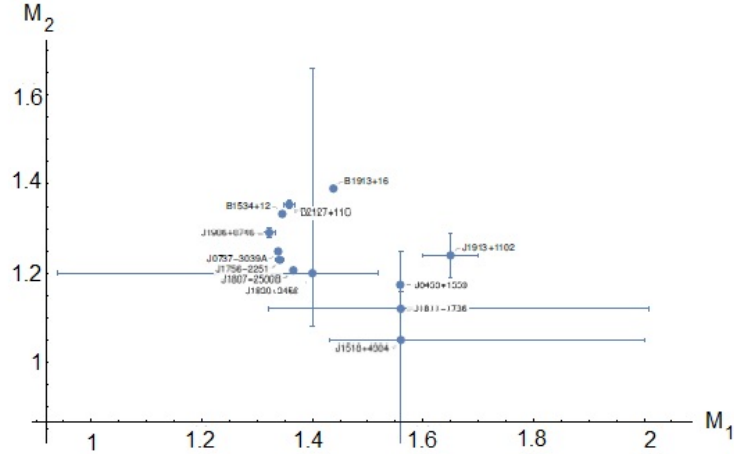


Fig. 1.8: Individual masses of Double neutron star systems.

We cannot, however, assume that NSs masses in binaries are strictly independent from each other. There are several mass transfer events on the stellar evolution that leads to such systems that will create a *correlation* between the two masses and other parameters, such as orbit periods and spins. Figure 1.8 suggest that in a general way, the greater m_1 , the lower m_2 . This shows that it would not be reasonable to use the same distribution as prior for both masses. Moreover, NSs in NS-WD systems for example, tend to be more massive than NSs in DNSs. We should not therefore treat them equally when estimating masses on DNS merging events, but focus the DNSs themselves. However, recent evidence of asymmetric DNS has raised a flag about the old belief in fully symmetric systems. And it is also important to remark that simulations obtained masses at birth in binary systems that are even higher than the ones determined for the two asymmetric DNS systems. The formation channel of the latter is still unknown and the small sample may contain observational biases.

With all these caveats, the time of a system to merge due to GW, τ , can be written as:

$$\tau = \frac{5}{264} \frac{a^4}{m^3} \frac{(1+q)^2}{q} \frac{1}{f(e)}, \quad (1.16)$$

where:

$$f(e) = \left[1 + \frac{73}{24}e^2 + \frac{37}{96}e^4 \right] [1 - e^2]^{-\frac{7}{2}}. \quad (1.17)$$

The parameter a is the semi major axis, m the total mass, and e the eccentricity of the orbit. Looking to Eq. (1.16) we can expect that systems with higher q will have a smaller τ , around 5%, which falls very shy from the observed on Fig. 1.9, where systems with higher q systematically have a smaller τ by several orders of magnitude.

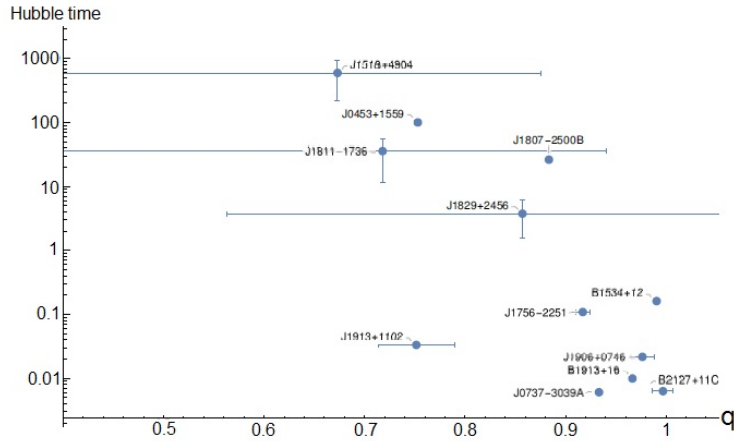


Fig. 1.9: Time to merge *vs* mass-ratio. The graphic shows the correlation between the time to merger due to gravitation waves τ and the mass quotient q . Systems with low q tend to have a higher τ .

It is still unclear why the observed DNSs display these correlations, and whether they can be generalized to all systems. As we discover new DNSs the questions about the veracity of these correlations will be answered and further studies on binary evolution should explain the mechanisms behind them.

1.4.2 *Asymmetry in the systems GW170817 and GW190425*

Since the operation of the new interferometers, two events compatible with NS mergers had been observed. The first event, GW170817 had a luminous counterpart detected in various wavelengths from radio to gamma-rays. The observations of the electromagnetic spectrum was important for the determinations such as ejected mass, details of the nucleosynthesis and others. The gamma rays detection connected to the merger helped consolidate NS mergers as a major candidate to the source of gamma-ray bursts - although the detected GRB was longer and weaker than most sGRBs-. The chirp mass of GW170817 was found to be $\mathcal{M} = 1.186M_{\odot}$, which is consistent with parameters close to most of the known binary systems.

The second event of this class was GW190425, albeit without a luminous counterpart and with a chirp mass of $\mathcal{M} = 1.44M_{\odot}$. This chirp mass indicates a higher total mass than any known galactic DNS. The analysis of the spin suggested that the most probable total mass lies around $3.35M_{\odot}$, $0.45M_{\odot}$ above the most massive observed system (PSR J1913+1102). This suggests that the source had an ultra-tight orbit origin, invisible to radio pulsar surveys due to high Doppler smearing effects. Alternatively, it is possible that the event was *not* the merger of a DNS, but rather of a NS-BH system. This alternative would require a BH in the apparent mass gap between neutron stars and black hokes, with $2 - 3M_{\odot}$. These objects however were never observed and lack a solid Stellar Evolution understanding.

Abbott *et al.* (2019, 2020a) presented a Bayesian analysis for the individual masses of both events given two different priors for the spins, one of them considering the maximal spin allowed by any known EoS as the upper limit, and the other considering the maximal spin observed in galactic NSs.

The interval of masses obtained by these two different priors differ a lot from each other in both events. For the GW170817 the high-spin prior yields $m_1 \in (1.36, 1.89)M_{\odot}$ & $m_2 \in (1.00, 1.36)M_{\odot}$ while the low-spin prior yields $m_1 \in (1.36, 1.60)M_{\odot}$ & $m_2 \in (1.16, 1.36)M_{\odot}$ in the 90% confidence interval.

Figure 1.11a shows the individual masses determination by the spin chirp mass analysis for the event GW190425 and Figure 1.11b shows the comparison of the total mass estimation of the event with the known galactic DNSs. For the low spin prior we have $m_1 \in (1.60, 1.87)M_{\odot}$ and $m_2 \in (1.46, 1.69)M_{\odot}$, while for the high spin: $m_1 \in (1.61, 2.52)M_{\odot}$ and $m_2 \in (1.12, 1.68)M_{\odot}$.

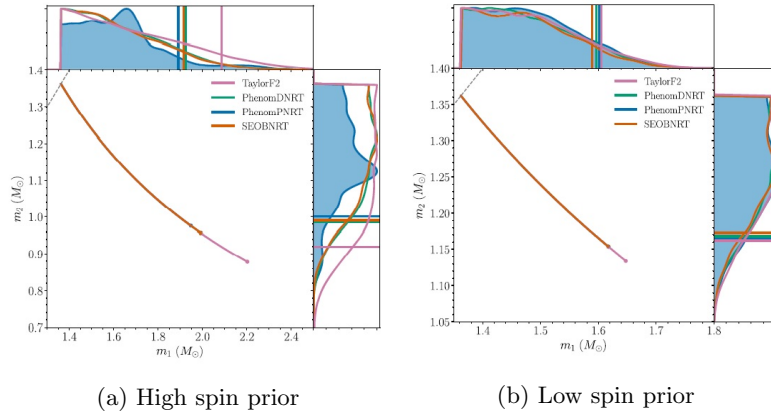


Fig. 1.10: Allowed masses interval from event GW170817 given different spin priors. Figure extracted from Abbott *et al.* (2019)

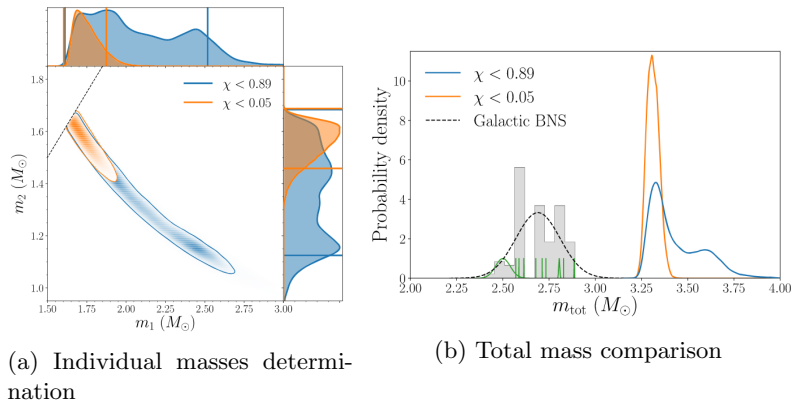


Fig. 1.11: Panel (a) shows the joint probability of individual masses of GW190425 for two different prior assumptions on the spin. Panel (b) compares the total mass of the event with the observed Galactic DNSs. Figure extracted from Abbott *et al.* (2019)

From the above description it is quite clear that GWs have opened a new era for NS physics, especially when combined with multiwavelength data as in the case of the merger GW170817. This “unseen” population is in many senses complementary to the information gathered from the known and yet-to-be-discovered nearby systems, and the joint study will produce

a positive feedback already apparent in the works that explore this issues.

1.5 Neutron star birth events

The birth of neutron stars has been generally associated to explosions of massive stars. This conviction stems from the pioneer work of Baade and Zwicky (1934), the link of the Crab pulsar with the 1054 A.D explosion (the latter itself not yet fully understood) and later association of several pulsars with supernova remnants (Tian and Leahy, 2004). While there are several reasons supporting this picture, it is not obvious that the formation of neutron stars cannot have contributions from other channels. The evidence regarding the mass distribution presented in Sec. 1.2 can help, when complemented with theoretical studies of massive stars and their very explosions (or failures) and alternative events which have been around for years, and that have been characterized much better in recent times (binary evolution and Accretion-Induced Collapse). We shall address these scenarios below and relate them to the empirical evidence as much as possible, in an attempt to complete with this topic an appraisal of the neutron star population origin as we understand today.

1.5.1 Neutron stars formed in single explosions

The evolution of single stars has produced a body of knowledge about their final fate which is relatively robust. In spite that several ingredients can modify somewhat the final numbers, it is generally agreed that the initial (ZAMS) mass and metallicity suffice to evolve the models and predict what the final outcome of the structure is, an important step towards the issue of NS formation itself. Figure 1.12 depicts the broad-brush picture of single star evolution. Atop the axis, the numbers indicate the masses of the stars at the ZAMS which produce the features indicated below the axis. For solar metallicity, assumed to be $Z = 0.01$, stars above $\sim 7.5M_{\odot}$ are the ones believed to be heavy enough to ignite carbon at their centers. This threshold is referred as M_{up} (or alternatively M_{CO}) in the literature. The minimum mass for the production of a neutron star after an explosive event is though to be slightly higher, at $M_n \sim 8M_{\odot}$ but with a higher uncertainty denoted with a question mark (M_{EC} is an alternative name for this quantity, stemming from “electron capture”). Finally, above $M_{\text{mass}} \geq 9M_{\odot}$ or so, depending on metallicity and input physics, all possible nuclear reactions are ignited and we enter the regime of “true” massive stars, developing an

iron core and exploding as a core collapse supernova (note the alternative names M_{crit} and M_{ccsn} also found in the literature for the same mass (Doherty *et al.*, 2017)). If the limits can not be made more precise is due to two main factors (although other ones also exist): the uncertainties in the mass loss rate in the advanced stages and the true nature of convection inside the progenitors. As mentioned, the metallicity is important for the location of the boundaries, and as a general trend we know that the figures are lower for lower metallicities, and even so a substantial spread in the calculations still exist (Doherty *et al.*, 2017).

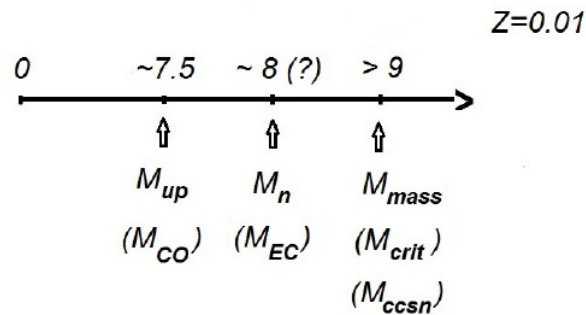


Fig. 1.12: The boundaries of mass (ZAMS) separating the different regimes for solar metallicity. The numbers above the axis denote the approximate locations of the separation between regimes, with their names and alternatives indicated below. See text for details.

While the actual problems above M_{mass} are mainly related to the collapse-implosion and launch of the supernova explosion, the fate of massive stars below M_{mass} presents a series of difficulties even before their final fate. The latest stage of these objects, characterized by the off-center ignition of degenerate carbon before the thermal pulses (TPs), is known as the “super-AGB” phase. Stars just below the M_n limit are thought to leave *O-Ne-Mg* white dwarfs, and those slightly less massive a *C-O-Ne* white dwarf, but without explosions involved. A true unsolved problem is that the super-AGB stars have never been identified observationally with confidence, and indeed they do not stand out clearly from neighbours at nearby positions in the HR diagram. Consequently, we must rely on the accurateness of theoretical calculations for the determination of M_{up} and related quantities.

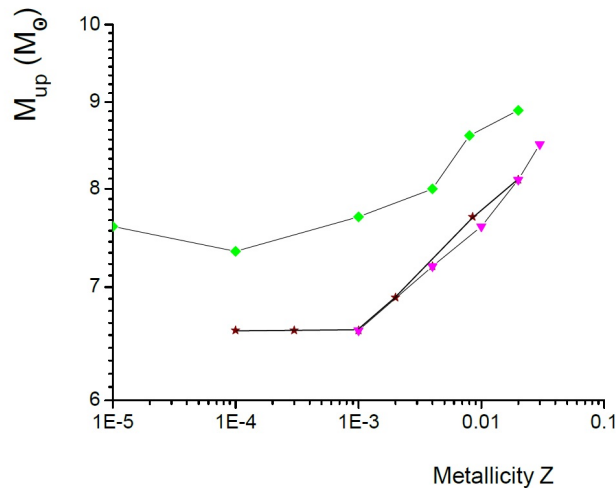


Fig. 1.13: Sample calculations of the quantities M_{up} as a function of the metallicity Z . The three curves correspond to the calculations of Siess (2007) (diamonds, upper), Doherty *et al.* (2015) (stars, middle) and Umeda *et al.* (1999) (triangles, lower)

A second important mass scale starts at a value M_n , above which the cores may undergo electron captures and explode as a class of supernovae, forming neutron stars. The electron-capture supernovae start with the reduction of the electron fraction per baryon Y_e because of capture reactions onto Mg and Ne , followed by pressure support loss and collapse of the core having a quite *fixed value* of mass, $1.375M_{\odot}$. The explosion receives a massive contribution from the energy released by oxygen burning in nuclear statistical equilibrium, and therefore the event is actually close to a Type Ia thermonuclear event (a recent claim of the identification of an electron-capture supernova showing all the expected features has been presented by Hiramatsu (2020)). Because of this features, it is believed that an almost-fixed mass neutron star is formed, with $m \sim 1.25M_{\odot}$ which results from the emission of the binding energy of the fixed core. Since this mass range is the most abundant among the exploding progenitors, it is expected that they make a large fraction of the full supernova rate, as it is easily seen from the form of the IMF function. Because of these features, it is expected that a group of “light” neutron stars stands out in the mass distribution (Schwab *et al.*, 2010), although confirming its presence may still be statistically

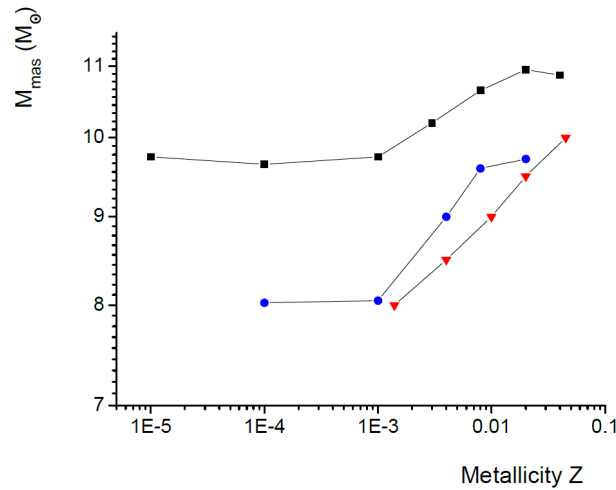


Fig. 1.14: Sample calculations of the quantities M_{mass} as a function of the metallicity Z . The curves are due to Siess (2007) (squares, upper), Doherty *et al.* (2015) (dots, middle) and Eldridge and Tout (2004) (triangles, lower).

tricky and would require a larger sample (Rocha *et al.*, 2019), as stated in Section 1.

The discussion above implicitly requires that if even *lighter* ($< 1.25M_{\odot}$) neutron stars exist, they must be formed in the explosion of small *iron* cores, not the ones undergoing the electron-capture supernovae. In other words, it is important to determine both the smallest neutron star mass and the lightest iron core resulting from the evolution of a $M \sim M_{\text{mass}}$ star. From the observation's diagram shown in Sec. 1.2, we identify the masses of PSR J1453+1559 companion, with $1.174 \pm 0.004M_{\odot}$ as the lightest exactly measured neutron star. Other sources such as 4U1538-522 and Her X-1 may also be considered, but their error bars are larger and must be refined. With this figure for the gravitational mass M_G , the iron core progenitor of this low-mass neutron star should have been no heavier than $\sim 1.28M_{\odot}$. Generally speaking, it is easier to find the baryonic masses of the remnants M_B than the gravitational mass M_G in the literature. The difference of both quantities, related to the binding energy, has to be calculated for each underlying theory of gravitation. However, a simple approximate expression for the latter quantity has been found by Lattimer and Prakash (2001) in terms of the quantity $\beta = GM_G/c^2R_0$, where G is Newton's constant, c the

speed of light and R_0 a fiducial radius (safely set to 12km) to relate both quantities quite accurately, namely:

$$\frac{M_B - M_G}{M_G} = 0.6 \frac{\beta}{1 - 0.5\beta} \quad (1.18)$$

and can be used quite safely if an extreme accuracy is not required.

The simulation of explosions of single stars have found confronting results for the minimum iron core forming the lightest neutron stars. For instance, Timmes *et al.* (1996) found a small number of progenitors that can produce a $M_G \leq 1.2M_\odot$. A more recent work by Sukhbold *et al.* (2016), calibrated for two progenitors, does not produce any neutron star below $M_G = 1.2M_\odot$. A dedicated study of the iron core at the onset of collapse (Suwa *et al.*, 2018), formed by low-mass *CO* cores has obtained “light” neutron stars in the mass range of the observed sources, and even close to $\sim 1M_\odot$. This is consistent with the results of Ugliano *et al.* (2012), in which a minimum baryonic mass of $\sim 1.2M_\odot$ would render suitable gravitational mass after applying Eq. (1.7) (although for a quite narrow mass range of the progenitors). All these works and a few others are quite difficult to compare because of different prescriptions for the stellar physics, different pre-supernova models and different numerical codes. In any case, it is entirely possible that a single star explosion does not constitute a valid evaluation for this lower limit, since the systems are found in binaries and binary stellar evolution is likely important. We shall return to this point in the next section.

With all the above caveats, it is fair to state that theoretical model explosions are not at odds with the empirical mass distribution found in Sec. 1.2. However, all the simulations produce stellar remnants which could be associated with the “second peak” around $1.8M_\odot$, but fall short of explaining the higher masses detected in actual systems. An example of this statement can be seen in Figure 1.15, and similar features are present in other works. Naively one could have expected that the jump in the size of iron core above $\sim 19M_\odot$ could be the reason for the production of heavy neutron stars, and even if this is true, the final values of the neutron stars M_G does not go above $1.9M_\odot$. The reason for these large iron cores, often overlooked in general works, is that there is a finite entropy inside them, making the “effective” Chandrasekhar mass $M_{\text{Ch,eff}}$ to grow from its cold value $M_{\text{Ch,0}}$ according to Timmes *et al.* (1996):

$$M_{\text{Ch,eff}} \simeq M_{\text{Ch},0} \left(1 + \left(\frac{s_e}{\pi Y_e} \right)^2 \right) \quad (1.19)$$

where, inserting a rough average for the electronic entropy per baryon $\langle s_e \rangle = 1$ and given that $Y_e \geq 0.4$ in general, produces collapsing cores of $\sim 1.8M_\odot$. However, in spite of this growth, the iron cores never reach values well above $2M_\odot$, that would be necessary to reproduce the highest measured neutron star masses. A contrasting view has been recently presented by Burrows and Vartanyan (2020), which in a summary of their present and former simulations were able to obtain not only explosions, but also gravitational masses up to $\sim 2M_\odot$ for remnant neutron stars. There is some important factor(s) not yet understood in the systematics of collapse simulations obtained by different groups to firmly assert whether high masses above $\sim 2M_\odot$ can be produced by this formation channel at birth, or and/or subsequent accretion is needed to reach the highest observed values. This statement is also important for massive pulsars with $\geq 2M_\odot$, which have been suggested to be born “as is” (Deng *et al.*, 2020), without suffering substantial accretion: if this happens to be true, current models of the explosions should obtain them.

As a general trend we see that the simulations do well to reproduce the “first” peak around $1.35 - 1.4M_\odot$ and can populate the “second peak” as well. It is the high-mass tail definitely present in the distribution that is not obtained. In addition, the presence of a “low-mass” peak is quite interesting and worth mentioning. We have stated that since light-mass ZAMS progenitors are very abundant, it is expected that presence of $\sim 1.25M_\odot$ can be easily seen. There are definitely a group of neutron stars in the histogram that were identified as such (Schwab *et al.*, 2010), but they are often “merged” with the main “first peak” using statistical discriminators (Section 1). In other words, even though their presence is possible, it has a low probability from this point of view (Horvath and Valentim, 2016). Moreover, it is intriguing that, even *ignoring* the electron-capture events, a peak at that position has been obtained by Sukhbold *et al.* (2016). Therefore, we find somewhat counter-intuitive that the statistical significance of this group is not higher than the presently obtained one.

Finally, we would like to point out that a substantial advance in the knowledge of the connection between events and NS masses has a long road ahead. It is clear that the attack to this problem produced a lot of advances, and revealed an extreme complexity that is still being deciphered. One of

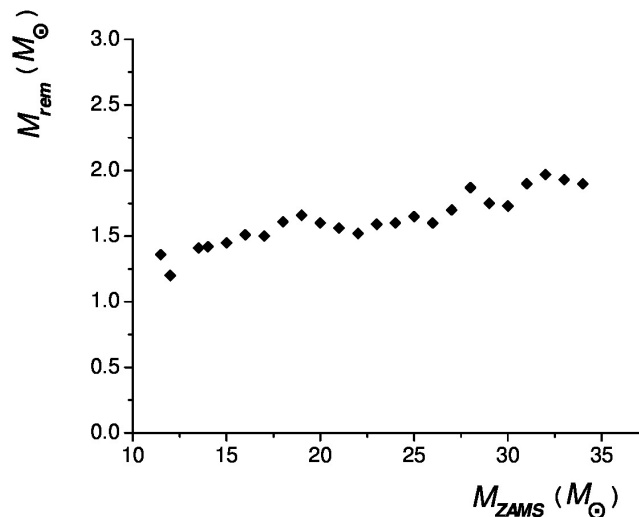


Fig. 1.15: The compact remnants of single star explosions (baryonic mass) obtained by as a function of the ZAMS progenitor mass((Ugliano *et al.*, 2012)).

the major issues, in our view, will be to establish whether the formation of NS and BH is monotonic (Burrows and Vartanyan (2020)) or “intermittent” (Sukhbold *et al.* (2016)), and which are the conditions for that behavior.

1.5.2 Neutron stars formed in binaries

Neutron stars are known to be present in a variety of systems. Some of them required quite sophisticated models for the evolution of a binary system featuring several phases along its life. Therefore the question of a *binary* neutron star origin, in contrast with the isolated single-star evolution discussed above arises.

The full evolution of stars in binary systems is not yet calculated until the *CO* core forms. This means that the pre-supernova structure is not really known, but rather assumed using reasonable prescriptions. It is generally assumed that the whole consequence of binary interaction is to promptly remove the entire hydrogen envelope of the star at helium ignition (Ertl *et al.*, 2020). The exact amount of accurateness of this simplification is not known, although it is a very reasonable first attempt and does not seem to imply any obvious misbehavior. An attempt to improve the situation

can be seen in the work by Patton and Sukhbold (2020).

Works using some version of this simple stripping hypothesis have been presented, with exploding “helium star” masses ranging from ≥ 1 to $40M_{\odot}$ since the removal of the envelope is a common feature of almost all close binary system evolution, the relation of the final iron core mass with the initial M_{ZAMS} is uncertain, because it depends on the mass loss rate, and even the specific code results need to be validated. Nevertheless, the neutron star distribution presents some features which are not present in the single-star explosions. For example, Woosley *et al.* (2020) obtain some objects that, because of larger fallback, lie above the $2M_{\odot}$ mark for all the mass-loss prescriptions. Ertl *et al.* (2020) also obtain a small fraction of heavy objects. In both cases the synthesis of a bimodal (or even trimodal) population presented in section Sec. 1.2 remains to be demonstrated in detail. The production of stars with $M_G \leq 1.2M_{\odot}$ does not appear to be favored in these simulations. However, the work of Fortin *et al.* (2016) claims to produce neutron stars as light as $\sim 1M_{\odot}$, although their framework is difficult to compare with the former.

Given that there are many systems in which the interaction of both components inevitably leads to consider the issue of the explosion(s) themselves, it is likely that substantial advances can be made in the near future, once the pre-collapse structure can be determined (Patton and Sukhbold, 2020). One prime example is the well-known path towards binary neutron stars (see, for example, Tauris *et al.* (2017); van den Heuvel (2018)) in which a detailed evolution implying “ultra-stripped” supernovae is needed. To connect with the issue of the NS distribution, we should state that even if the binary neutron stars that originated the “ $1.4M_{\odot}$ paradigm” have not accreted substantially after formation, no real reason to expect a “fixed mass” exists. In fact, recent observations of *asymmetric* binary neutron star systems (Ferdman *et al.*, 2020) that can merge on less than a Hubble time may call for a reanalysis of the masses at birth, in line with the simulation work just described. On the other hand, BH production with a supernova explosion has been also found possible, and in fact a recent report Maxted *et al.* (2020) claims one of these identifications.

1.5.3 *The Accretion-Induced Collapse channel for NS formation*

The process by which a white dwarf can collapse and form a neutron star, known as Accretion-Induced Collapse (AIC), has been present for more

than 40 yrs and invoked to solve a large variety of problems in stellar astrophysics. The basic original idea is that for white dwarfs near their own Chandrasekhar limit, a high accretion rate \dot{M} (but below the Eddington limit) from a MS or RG companion can make the electron captures more efficient than the thermonuclear ignition of carbon or even oxygen, triggering the collapse of the star by removing the degenerate electron pressure (see, for example, Nomoto and Kondo (1991)). Theoretically, AIC events could be quite frequent and originate neutron stars in many binary systems. In fact, the detection of a large number of low-mass binary pulsars in globular clusters was one of the features in which AIC was suggested to operate (Grindlay and Bailyn, 1988). AIC has been also invoked in the magnetar formation problem (Margalit *et al.*, 2019), expecting a flux-conservation amplification of an initial magnetic field of the white dwarf, and many other systems like intermediate-mass and millisecond pulsars. A “double degenerate” AIC resulting from the merging of two white dwarfs with a short orbital period was later discussed as a complementary possibility to the “single degenerate” channel, analogously to the problem of Type Ia supernova progenitors to which they have a kinship.

Since we are concerned with the neutron star formation from these events only, we just point out what are the results and expectations relevant for our subject. The first important observation is that the very events have never been positively identified, although it is expected that their luminosity remains low, and therefore this is not a big surprise. The first detailed calculation of the AIC (Fryer *et al.*, 1999) obtained an important output of exotic isotopes in the $\sim 0.1M_{\odot}$ ejecta, and proceed to deduce an upper limit to the occurrence in the galaxy based on the measured abundance of them. This exotic isotope production has been challenged by Qian and Wasserburg (2007), and makes the issue of the upper limit uncertain. On the other hand, population synthesis have yielded the expectation of $\sim 10^7$ pulsars formed by AIC in the single-degenerate channel and a few times this figure coming from the double-degenerate channel (Wang and Liu, 2020). This are high numbers and may be in tension with the estimated rate of $\leq 0.1\%$ of the total neutron star population estimated by Fryer *et al.* (1999). If the overproduction of exotic isotopes can be avoided, high rates could be eventually accepted. The alternative way out of this quandary is that the number of suitable progenitor systems is overestimated, and that AIC neutron stars will not produced in many of the current candidates mergings, but which of these solutions is viable remains unsolved for the present.

The production of neutron stars in the single-degenerate channel would

be in a narrow range around $1.25M_{\odot}$ naively, but models envisage the accretion to resume after their formation. Therefore, the actual range of the neutron star masses may extend all the way up to the highest measured masses if the accretion conditions allows it. For the double-degenerate channel, the expected range is different, and is believed to span the range $1.4 - 2.8M_{\odot}$, with a slight variation according to the chemical composition of the white dwarfs (Wang and Liu, 2020). We note that this may be an efficient way to form extremely heavy neutron stars “at birth”, a feature that may be required if more heavy objects are detected. The contribution of GW observations to this task is very important, as suggested by the detection of a $2.6M_{\odot}$ object in the merge GW190814 (Abbott *et al.*, 2020c), although the true nature of this component remains to be confirmed, as stated in Sec. 1.4.

1.6 Conclusions

The study of neutron star origins and masses has entered a mature age, with a growing body of reliable data and perspectives to clarify the basic facts of these amazing objects. The main points discussed above can be summarized as follows:

- Contrary to earlier beliefs, there is no “canonical” neutron star mass. The most abundant NSs in the sample do have masses around this value, but a substantial fraction of the sample is either smaller or much larger than that, possibly up to $\sim 1M_{\odot}$ heavier.
- The situation with the so-called “mass gap”, closely related to the M_{TOV} issue and the mechanism(s) of formation, is not clear yet. A “gap” has been reported in the merging GW events. The presence of “light” (i.e. $3M_{\odot}$) black holes is not certain, although this may still be due to detection biases and could be associated to the light components in a few GW mergings. It is important to keep looking for them in local systems.
- Theoretical models of NS must produce high masses, maybe closer to the Rhoades-Ruffini limit than we use to think a few years ago.
- The study of merging NS-NS and possibly NS-BH mergers could prove crucial for the determination of M_{TOV} and the mass ratio of the binaries, while the studies of local systems are complementary and amenable to more direct analysis.
- Supernova simulations are now on a full different level of sophistication,

and had achieved some important goals. However, there are still differences between the results of different groups that are important for our main focus. It is still not clear whether heavy NS with $M \geq 2M_{\odot}$ can be formed directly, and the issue of monotonicity of the NS-BH remnants with the remnant mass and other relevant factors (binarity, treatment of pre-SN physics, etc.) does not seem fully established.

- The existence of NSs with mass significantly below $1.25M_{\odot}$ may be interpreted as empirical evidence for small iron cores. It is important for Stellar Evolution to determine this low-end of the distribution of masses.

Acknowledgements

JEH wishes to acknowledge the financial support of the Fapesp Agency (São Paulo) through the grant 13/26258-4 and the CNPq (Federal Government) for the award of a Research Fellowship. The CAPES Agency (Federal Government) is acknowledged for financial support in the form of Scholarships.

Bibliography

- Abbott, B., Abbott, R., Abbott, T., Abraham, S., Acernese, F., Ackley, K., Adams, C., Adhikari, R., Adya, V., *et al.* (2020a). Gw190425: Observation of a compact binary coalescence with total mass $3.4m_{\odot}$, *The Astrophysical Journal Letters* **892**, pp. L3–L6.
- Abbott, B., Abbott, R., Abbott, T., Acernese, F., Ackley, K., Adams, C., Adams, T., Addesso, P., Adhikari, R., Adya, V., *et al.* (2019). Properties of the binary neutron star merger gw170817, *Physical Review X* **9**, p. 011001.
- Abbott, B. P., Abbott, R., Abbott, T., Abernathy, M., Acernese, F., Ackley, K., Adams, C., Adams, T., Addesso, P., Adhikari, R., *et al.* (2016a). Properties of the binary black hole merger gw150914, *Physical Review Letters* **116**, p. 241102.
- Abbott, B. P., Abbott, R., Abbott, T., Abernathy, M., Acernese, F., Ackley, K., Adams, C., Adams, T., Addesso, P., *et al.* (2016b). Observation of gravitational waves from a binary black hole merger, *Physical Review Letters* **116**, p. 061102.
- Abbott, R., Abbott, T., Abraham, S., Acernese, F., Ackley, A., Adams, A., *et al.* (2020b). Population properties of compact objects from the second ligo–virgo gravitational-wave transient catalog, *arXiv preprint arXiv:2010.14533v1*.
- Abbott, R., Abbott, T., Abraham, S., Acernese, F., Ackley, K., Adams, C., Adhikari, R., Adya, V., Affeldt, C., Agathos, M., *et al.* (2020c). Gw190814: gravitational waves from the coalescence of a $23 m_{\odot}$ black hole with a $2.6 m_{\odot}$ compact object, *The Astrophysical Journal Letters* **896**, pp. L44–L47.
- Ai, S., Gao, H., and Zhang, B. (2020). What constraints on the neutron star maximum mass can one pose from gw170817 observations? *The Astrophysical Journal* **893**, p. 146.
- Akmal, A. and Pandharipande, V. R. (1997). Spin-isospin structure and pion condensation in nucleon matter, *Physical Review C* **56**, p. 2261.
- Alcock, C., Farhi, E., and Olinto, A. (1986). Strange stars, *The Astrophysical Journal* **310**, pp. 261–272.
- Alford, M., Braby, M., Paris, M., and Reddy, S. (2005). Hybrid stars that masquerade as neutron stars, *The Astrophysical Journal* **629**, pp. 969–978.

- Alsing, J., Silva, H. O., and Berti, E. (2018). Evidence for a maximum mass cut-off in the neutron star mass distribution and constraints on the equation of state, *Monthly Notices of the Royal Astronomical Society* **478**, pp. 1377–1391.
- Antoniadis, J., Freire, P. C., Wex, N., Tauris, T. M., Lynch, R. S., van Kerkwijk, M. H., Kramer, M., Bassa, C., Dhillon, V. S., Driebe, T., *et al.* (2013). A massive pulsar in a compact relativistic binary, *Science* **340**, 6131.
- Antoniadis, J., Tauris, T. M., Ozel, F., Barr, E., Champion, D. J., and Freire, P. C. (2016). The millisecond pulsar mass distribution: Evidence for bimodality and constraints on the maximum neutron star mass, *arXiv preprint arXiv:1605.01665* .
- Antoniadis, J., Van Kerkwijk, M., Koester, D., Freire, P., Wex, N., Tauris, T., Kramer, M., and Bassa, C. (2012). The relativistic pulsar–white dwarf binary psr j1738+ 0333–i. mass determination and evolutionary history, *Monthly Notices of the Royal Astronomical Society* **423**, pp. 3316–3327.
- Arzoumanian, Z., Brazier, A., Burke-Spolaor, S., Chamberlin, S., Chatterjee, S., Christy, B., Cordes, J. M., Cornish, N. J., Crawford, F., Cromartie, H. T., *et al.* (2018). The nanograv 11-year data set: high-precision timing of 45 millisecond pulsars, *The Astrophysical Journal Supplement Series* **235**, p. 37.
- Baade, W. and Zwicky, F. (1934). On super-novae, *Proceedings of the National Academy of Sciences* **20**, pp. 254–259.
- Babu, G. J. and Feigelson, E. D. (2006). Astrostatistics: Goodness-of-Fit and All That! in C. Gabriel, C. Arviset, D. Ponz, and S. Enrique (eds.), *Astronomical Data Analysis Software and Systems XV*, *Astronomical Society of the Pacific Conference Series*, Vol. 351, pp. 127–137.
- Barr, E., Freire, P., Kramer, M., Champion, D., Berezhina, M., Bassa, C., Lyne, A., and Stappers, B. (2017). A massive millisecond pulsar in an eccentric binary, *Monthly Notices of the Royal Astronomical Society* **465**, pp. 1711–1719.
- Bassa, C., Van Kerkwijk, M., Koester, D., and Verbunt, F. (2006). The masses of psr j1911–5958a and its white dwarf companion, *Astronomy & Astrophysics* **456**, pp. 295–304.
- Baym, G., Pethick, C., and Sutherland, P. (1971). The ground state of matter at high densities: equation of state and stellar models, *The Astrophysical Journal* **170**, pp. 299–310.
- Benvenuto, O. and Horvath, J. (1989). On the structure of strange stars and bagged qcd parameters, *Monthly Notices of the Royal Astronomical Society* **241**, pp. 43–50.
- Benvenuto, O. G., De Vito, M. A., and Horvath, J. (2012). Evolutionary trajectories of ultracompact “black widow” pulsars with very low mass companions, *The Astrophysical Journal Letters* **753**, p. L33.
- Benvenuto, O. G., De Vito, M. A., and Horvath, J. E. (2014). Understanding the evolution of close binary systems with radio pulsars, *The Astrophysical Journal Letters* **786**, p. L7.
- Berezhina, M., Champion, D., Freire, P., Tauris, T., Kramer, M., Lyne, A., Stap-

- pers, B., Guillemot, L., Cognard, I., Barr, E., *et al.* (2017). The discovery of two mildly recycled binary pulsars in the northern high time resolution universe pulsar survey, *Monthly Notices of the Royal Astronomical Society* **470**, pp. 4421–4433.
- Bhalerao, V. B. (2012). *Neutron Stars and NuSTAR: A Systematic Survey of Neutron Star Masses in High Mass X-ray Binaries and Characterization of CdZnTe Detectors for NuSTAR* (Universal-Publishers, USA).
- Bhat, N. R., Bailes, M., and Verbiest, J. P. (2008). Gravitational-radiation losses from the pulsar–white-dwarf binary psr j1141–6545, *Physical Review D* **77**, p. 124017.
- Bodmer, A. (1971). Collapsed nuclei, *Physical Review D* **4**, p. 1601.
- Breu, C. and Rezzolla, L. (2016). Maximum mass, moment of inertia and compactness of relativistic stars, *Monthly Notices of the Royal Astronomical Society* **459**, pp. 646–656.
- Burrows, A. and Vartanyan, D. (2020). Core-collapse supernova explosion theory, *arXiv:2009.14157*.
- Casares, J., Hernández, J. G., Israelian, G., and Rebolo, R. (2010). On the mass of the neutron star in cyg x-2, *Monthly Notices of the Royal Astronomical Society* **401**, pp. 2517–2520.
- Chamel, N., Haensel, P., Zdunik, J. L., and Fantina, A. (2013). On the maximum mass of neutron stars, *International Journal of Modern Physics E* **22**, p. 1330018.
- Cromartie, H. T., Fonseca, E., Ransom, S. M., Demorest, P. B., Arzoumanian, Z., Blumer, H., Brook, P. R., DeCesar, M. E., Dolch, T., Ellis, J. A., *et al.* (2020). Relativistic shapiro delay measurements of an extremely massive millisecond pulsar, *Nature Astronomy* **4**, pp. 72–76.
- de Avellar, M. G. and Horvath, J. (2010). Exact and quasi-exact models of strange stars, *International Journal of Modern Physics D* **19**, pp. 1937–1955.
- Deller, A., Archibald, A., Brisken, W., Chatterjee, S., Janssen, G., Kaspi, V., Lorimer, D., Lyne, A., McLaughlin, M., Ransom, S., *et al.* (2012). A parallax distance and mass estimate for the transitional millisecond pulsar system j1023+ 0038, *The Astrophysical Journal Letters* **756**, pp. L25–L28.
- Demorest, P. B., Pennucci, T., Ransom, S., Roberts, M., and Hessels, J. (2010). A two-solar-mass neutron star measured using shapiro delay, *Nature* **467**, 7319, pp. 1081–1083.
- Deneva, J. S., Freire, P., Cordes, J., Lyne, A., Ransom, S., Cognard, I., Camilo, F., Nice, D. J., Stairs, I., Allen, B., *et al.* (2012). Two millisecond pulsars discovered by the palf survey and a shapiro delay measurement, *The Astrophysical Journal* **757**, p. 89.
- Deng, Z.-L., Gao, Z.-F., Li, X.-D., and Shao, Y. (2020). On the formation of psr j1640+2224: A neutron star born massive? *The Astrophysical Journal* **892**, p. id.4.
- Desvignes, G., Caballero, R., Lentati, L., Verbiest, J., Champion, D., Stappers, B., Janssen, G., Lazarus, P., Osłowski, S., Babak, S., *et al.* (2016). High-precision timing of 42 millisecond pulsars with the european pulsar timing array, *Monthly Notices of the Royal Astronomical Society* **458**, pp. 3341–

- 3380.
- Doherty, C. L., Gil-Pons, P., Siess, L., and Lattanzio, J. C. (2017). Super-agb stars and their role as electron capture supernova progenitors, *Publications of the Astronomical Society of Australia* **34**, p. e056.
- Doherty, C. L., Gil-Pons, P., Siess, L., Lattanzio, J. C., and Lau, H. H. B. (2015). Super- and massive agb stars - iv. final fates - initial-to-final mass relation, *Monthly Notices of the Royal Astronomical Society* **446**, pp. 2599–2612.
- Douchin, F. and Haensel, P. (2001). A unified equation of state of dense matter and neutron star structure, *Astronomy & Astrophysics* **380**, pp. 151–167.
- Eldridge, J. J. and Tout, C. A. (2004). The progenitors of core-collapse supernovae, *Monthly Notices of the Royal Astronomical Society* **353**, pp. 87–97.
- Engvik, L., Hjorth-Jensen, M., Osnes, E., Bao, G., and Østgaard, E. (1994). Asymmetric nuclear matter and neutron star properties, *Physical Review Letters* **73**, p. 2650.
- Ertl, T., Woosley, S. E., Sukhbold, T., and Janka, H.-T. (2020). The explosion of helium stars evolved with mass loss, *The Astrophysical Journal* **890**, p. 51.
- Falanga, M., Bozzo, E., Lutovinov, A., Bonnet-Bidaud, J., Fetisova, Y., and Puls, J. (2015). Ephemeris, orbital decay, and masses of ten eclipsing high-mass x-ray binaries, *Astronomy & Astrophysics* **577**, p. A130.
- Farrow, N., Zhu, X.-J., and Thrane, E. (2019). The mass distribution of galactic double neutron stars, *The Astrophysical Journal* **876**, p. 18.
- Ferdman, R., Freire, P., Perera, B., Pol, N., Camilo, F., Chatterjee, S., Cordes, J., Crawford, F., Hessels, J., Kaspi, V., *et al.* (2020). Asymmetric mass ratios for bright double neutron-star mergers, *Nature* **583**, 7815, pp. 211–214.
- Ferdman, R. D., Stairs, I. H., Kramer, M., Janssen, G. H., Bassa, C. G., Stappers, B. W., Demorest, P. B., Cognard, I., Desvignes, G., Theureau, G., *et al.* (2014). PSR J1756-2251: a pulsar with a low-mass neutron star companion, *Monthly Notices of the Royal Astronomical Society* **443**, pp. 2183–2196.
- Ferdman, R. D., Stairs, I. H., Kramer, M., McLaughlin, M. A., Lorimer, D. R., Nice, D. J., Manchester, R. N., Hobbs, G., Lyne, A. G., Camilo, F., *et al.* (2010). A precise mass measurement of the intermediate-mass binary pulsar PSR J1802-2124, *The Astrophysical Journal* **711**, p. 764.
- Finn, L. S. (1994). Observational constraints on the neutron star mass distribution, *Physical Review Letters* **73**, p. 1878.
- Fonseca, E., Pennucci, T. T., Ellis, J. A., Stairs, I. H., Nice, D. J., Ransom, S. M., Demorest, P. B., Arzoumanian, Z., Crowter, K., Dolch, T., *et al.* (2016). The nanograv nine-year data set: mass and geometric measurements of binary millisecond pulsars, *The Astrophysical Journal* **832**, pp. 167–180.
- Fonseca, E., Stairs, I. H., and Thorsett, S. E. (2014). A comprehensive study of relativistic gravity using PSR B1534+12, *The Astrophysical Journal* **787**, p. 82.
- Fortin, M., Bejger, M., Haensel, P., and Zdunik, J. (2016). Progenitor neutron stars of the lightest and heaviest millisecond pulsars, *Astronomy & Astrophysics* **586**, p. A109.
- Franzoni, B., Fogaça, D. A., Navarra, F. S., and Horvath, J. E. (2012). Self-bound interacting QCD matter in compact stars, *Physical Review D* **86**, p. 065031.

- Freire, P., Bassa, C., Wex, N., Stairs, I., Champion, D., Ransom, S., Lazarus, P., Kaspi, V., Hessels, J., Kramer, M., *et al.* (2011). On the nature and evolution of the unique binary pulsar j1903+ 0327, *Monthly Notices of the Royal Astronomical Society* **412**, pp. 2763–2780.
- Freire, P. C., Wolszczan, A., van den Berg, M., and Hessels, J. W. (2008). A massive neutron star in the globular cluster m5, *The Astrophysical Journal* **679**, p. 1433.
- Fruchter, A., Stinebring, D., and Taylor, J. (1988). A millisecond pulsar in an eclipsing binary, *Nature* **333**, 6170, pp. 237–239.
- Fryer, C., Benz, W., Herant, M., and Colgate, S. A. (1999). What can the accretion-induced collapse of white dwarfs really explain? *The Astrophysical Journal* **516**, p. 892.
- Glendenning, N. K. (1985). Neutron stars are giant hypernuclei? *The Astrophysical Journal* **293**, pp. 470–493.
- Glendenning, N. K. (2012). *Compact stars: Nuclear physics, particle physics and general relativity* (Springer Science & Business Media, Berlin).
- Grindlay, J. and Bailyn, C. (1988). Birth of millisecond pulsars in globular clusters, *Nature* **336**, 6194, pp. 48–50.
- Haensel, P. and Pichon, B. (1993). Experimental nuclear masses and the ground state of cold dense matter, *arXiv preprint nucl-th/9310003*.
- Haensel, P., Potekhin, A. Y., and Yakovlev, D. G. (2007). *Neutron stars 1: Equation of state and structure*, Vol. 326 (Springer Science & Business Media, Berlin).
- Haseltine, E. (2002). The 11 greatest unanswered questions of physics, *DISCOVER-NEW YORK* **23**, 2, pp. 36–43.
- Heger, A., Fryer, C., Woosley, S., Langer, N., and Hartmann, D. H. (2003). How massive single stars end their life, *The Astrophysical Journal* **591**, p. 288.
- Heiselberg, H. and Pandharipande, V. (2000). Recent progress in neutron star theory, *Annual Review of Nuclear and Particle Science* **50**, pp. 481–524.
- Hewish, A., Bell, S. J., Pilkington, J. D., Scott, P. F., and Collins, R. A. (1968). Observation of a rapidly pulsating radio source, *Nature* **217**, 5130, pp. 709–713.
- Hiramatsu, D. e. a. (2020). The electron-capture origin of supernova 2018zd, .
- Horvath, J. (1996). Possible determination of isolated pulsar masses with gravitational microlensing, *Monthly Notices of the Royal Astronomical Society* **278**, pp. L46–L48.
- Horvath, J. (2007). What do exotic equations of state have to offer? in *Isolated Neutron Stars: From the Surface to the Interior* (Springer, Berlin), pp. 431–434.
- Horvath, J., Bernardo, A., Rocha, L., Valentim, R., Moraes, P., and de Avelar, M. (2020). Redback/black widow systems as progenitors of the highest neutron star masses and low-mass black holes, *SCIENCE CHINA Physics, Mechanics & Astronomy* **63**, p. id.129531.
- Horvath, J. E. and Valentim, R. (2016). The masses of neutron stars, *Handbook of Supernovae*, Eds. A.W. Alsabtu and P. Murdin, *arXiv:1607.06981*, pp. 1317–1329.

- Hui, C. Y. and Li, K. L. (2019). High energy radiation from spider pulsars, *Galaxies* **7**, p. 93.
- Hulse, R. A. and Taylor, J. H. (1975). Discovery of a pulsar in a binary system, *The Astrophysical Journal* **195**, pp. L51–L53.
- Jacoby, B. A., Cameron, P., Jenet, F., Anderson, S., Murty, R., and Kulkarni, S. (2006). Measurement of orbital decay in the double neutron star binary psr b2127+ 11c, *The Astrophysical Journal Letters* **644**, p. L113.
- Kaplan, D. L., Boyles, J., Dunlap, B. H., Tendulkar, S. P., Deller, A. T., Ransom, S. M., McLaughlin, M. A., Lorimer, D. R., and Stairs, I. H. (2014). A $1.05 m_{\odot}$ companion to psr j2222–0137: The coolest known white dwarf? *The Astrophysical Journal* **789**, p. 119.
- Kasian, L. E. (2012). *Radio observations of two binary pulsars*, Ph.D. thesis, University of British Columbia.
- Kiziltan, B., Kottas, A., De Yoreo, M., and Thorsett, S. E. (2013). The neutron star mass distribution, *The Astrophysical Journal* **778**, p. 66.
- Kramer, M., Stairs, I. H., Manchester, R., McLaughlin, M., Lyne, A., Ferdman, R., Burgay, M., Lorimer, D., Possenti, A., D’Amico, N., *et al.* (2006). Tests of general relativity from timing the double pulsar, *Science* **314**, 5796, pp. 97–102.
- Lackey, B. D., Nayyar, M., and Owen, B. J. (2006). Observational constraints on hyperons in neutron stars, *Physical Review D* **73**, p. 024021.
- Lattimer, J. and Prakash, M. (2001). Neutron star structure and the equation of state, *The Astrophysical Journal* **550**, p. 426.
- Lattimer, J. M. (2012). The nuclear equation of state and neutron star masses, *Annual Review of Nuclear and Particle Science* **62**, pp. 485–515.
- Linares, M. (2019). Super-massive neutron stars and compact binary millisecond pulsars, *arXiv preprint arXiv:1910.09572* .
- Lugones, G. and Arbañil, J. D. (2017). Compact stars in the braneworld: A new branch of stellar configurations with arbitrarily large mass, *Physical Review D* **95**, p. 064022.
- Lugones, G. and Horvath, J. (2002). Color-flavor locked strange matter, *Physical Review D* **66**, p. 074017.
- Lugones, G. and Horvath, J. (2003). High-density qcd pairing in compact star structure, *Astronomy & Astrophysics* **403**, pp. 173–178.
- Lynch, R. S., Freire, P. C., Ransom, S. M., and Jacoby, B. A. (2012). The timing of nine globular cluster pulsars, *The Astrophysical Journal* **745**, p. 109.
- Lyne, A. G., Burgay, M., Kramer, M., Possenti, R. N., A. and Manchester, Camilo, F., McLaughlin, M. A., *et al.* (2004). A double-pulsar system: A rare laboratory for relativistic gravity and plasma physics, *Science* **303**, pp. 1153–1157.
- Malaver, M. (2014). Strange quark star model with quadratic equation of state, *arXiv preprint arXiv:1407.0760* .
- Margalit, B., Berger, E., and Metzger, B. D. (2019). Fast radio bursts from magnetars born in binary neutron star mergers and accretion induced collapse, *The Astrophysical Journal* **886**, p. 110.
- Margalit, B. and Metzger, B. D. (2017). Constraining the maximum mass of

- neutron stars from multi-messenger observations of gw170817, *The Astrophysical Journal Letters* **850**, p. L19.
- Martinez, J., Stovall, K., Freire, P., Deneva, J., Jenet, F., McLaughlin, M., Bagchi, M., Bates, S., and Ridolfi, A. (2015). Pulsar j0453+ 1559: A double neutron star system with a large mass asymmetry, *The Astrophysical Journal* **812**, p. 143.
- Maxted, N. I., Ruiter, A. J., Belczynski, K., Seitenzahl, I. R., and Crocker, R. M. (2020). A supernova remnant associated with a nascent black hole low-mass x-ray binary, *arXiv preprint arXiv:2010.15341* .
- Müller, H. and Serot, B. D. (1996). Relativistic mean-field theory and the high-density nuclear equation of state, *Nuclear Physics A* **606**, pp. 508–537.
- Munoz-Darias, T., Casares, J., and Martínez-Pais, I. (2005). The “k-correction” for irradiated emission lines in lmxbs: Evidence for a massive neutron star in x1822–371 (v691 cra), *The Astrophysical Journal* **635**, p. 502.
- Müther, H., Prakash, M., and Ainsworth, T. (1987). The nuclear symmetry energy in relativistic brueckner-hartree-fock calculations, *Physics Letters B* **199**, pp. 469–474.
- Nice, D. J. (2003) (Cambridge University Press).
- Nomoto, K. (1984). Evolution of 8-10 solar mass stars toward electron capture supernovae. i-formation of electron-degenerate o+ ne+ mg cores, *The Astrophysical Journal* **277**, pp. 791–805.
- Nomoto, K. and Kondo, Y. (1991). Conditions for accretion-induced collapse of white dwarfs, *The Astrophysical Journal* **367**, pp. L19–L22.
- O’Boyle, M. F., Markakis, C., Stergioulas, N., and Read, J. S. (2020). A parametrized equation of state for neutron star matter with continuous sound speed, *arXiv preprint arXiv:2008.03342* .
- Oppenheimer, J. R. and Volkoff, G. M. (1939). On massive neutron cores, *Physical Review* **55**, p. 374.
- Özel, F. and Freire, P. (2016). Masses, radii, and the equation of state of neutron stars, *Annual Review of Astronomy and Astrophysics* **54**, pp. 401–440.
- Özel, F., Psaltis, D., Güver, T., Baym, G., Heinke, C., and Guillot, S. (2016). The dense matter equation of state from neutron star radius and mass measurements, *The Astrophysical Journal* **820**, p. 28.
- Özel, F., Psaltis, D., Narayan, R., and Villarreal, A. S. (2012). On the mass distribution and birth masses of neutron stars, *The Astrophysical Journal* **757**, p. 55.
- Patton, R. A. and Sukhbold, T. (2020). Towards a realistic explosion landscape for binary population synthesis, *arXiv preprint arXiv:2005.03055* .
- Podsiadlowski, P., Langer, N., Poelarends, A., Rappaport, S., Heger, A., and Pfahl, E. (2004). The effects of binary evolution on the dynamics of core collapse and neutron star kicks, *The Astrophysical Journal* **612**, p. 1044.
- Prakash, M., Cooke, J., and Lattimer, J. (1995). Quark-hadron phase transition in proton-neutron stars, *Physical Review D* **52**, p. 661.
- Qian, Y.-Z. and Wasserburg, G. (2007). Where, oh where has the r-process gone? *Physics Reports* **442**, pp. 237–268.
- Rajagopal, K. and Wilczek, F. (2001). The condensed matter physics of qcd, in

- At The Frontier of Particle Physics: Handbook of QCD (In 3 Volumes)* (World Scientific, Singapore), pp. 2061–2151.
- Ransom, S. M., Stairs, I., Archibald, A., Hessels, J., Kaplan, D., Van Kerkwijk, M., Boyles, J., Deller, A., Chatterjee, S., Schechtman-Rook, A., *et al.* (2014). A millisecond pulsar in a stellar triple system, *Nature* **505**, 7484, pp. 520–524.
- Rawls, M. L., Orosz, J. A., McClintock, J. E., Torres, M. A., Bailyn, C. D., and Buxton, M. M. (2011). Refined neutron star mass determinations for six eclipsing x-ray pulsar binaries, *The Astrophysical Journal* **730**, p. 25.
- Reardon, D., Hobbs, G., Coles, W., Levin, Y., Keith, M., Bailes, M., Bhat, N., Burke-Spolaor, S., Dai, S., Kerr, M., *et al.* (2016). Timing analysis for 20 millisecond pulsars in the parkes pulsar timing array, *Monthly Notices of the Royal Astronomical Society* **455**, pp. 1751–1769.
- Rezzolla, L., Most, E. R., and Weih, L. R. (2018a). Using gravitational-wave observations and quasi-universal relations to constrain the maximum mass of neutron stars, *The Astrophysical Journal Letters* **852**, p. L25.
- Rezzolla, L., Pizzochero, P., Jones, D. I., Rea, N., and Vidaña, I. (2018b). *The physics and astrophysics of neutron stars* (Springer, Berlin).
- Rhoades Jr, C. E. and Ruffini, R. (1974). Maximum mass of a neutron star, *Physical Review Letters* **32**, p. 324.
- Roberts, M. S. (2012). Surrounded by spiders! new black widows and redbacks in the galactic field, *Proceedings of the International Astronomical Union* **8**, S291, pp. 127–132.
- Rocha, L., Bernardo, A., De Avellar, M., and Horvath, J. (2020). Exact solutions for compact stars with cfl quark matter, *International Journal of Modern Physics D* **29**, p. id. 2050044.
- Rocha, L. S., Bernardo, A., Horvath, J. E., Valentim, R., and de Avellar, M. G. (2019). The distribution of neutron star masses, *Astronomische Nachrichten* **340**, pp. 957–963.
- Romani, R. W., Filippenko, A. V., Silverman, J. M., Cenko, S. B., Greiner, J., Rau, A., Elliott, J., and Pletsch, H. J. (2012). Psr j1311–3430: a heavy-weight neutron star with a flyweight helium companion, *The Astrophysical Journal Letters* **760**, p. L36.
- Ruderman, M. (1972). Pulsars: structure and dynamics, *Annual Review of Astronomy and Astrophysics* **10**, pp. 427–476.
- Ruiter, A., Ferrario, L., Belczynski, K., Seitenzahl, I., Crocker, R., and Karakas, A. (2019). On the formation of neutron stars via accretion-induced collapse in binaries, *Monthly Notices of the Royal Astronomical Society* **484**, pp. 698–711.
- Ruiz, M., Shapiro, S. L., and Tsokaros, A. (2018). Gw170817, general relativistic magnetohydrodynamic simulations, and the neutron star maximum mass, *Physical Review D* **97**, p. 021501.
- Schwab, J., Podsiadlowski, P., and Rappaport, S. (2010). Further evidence for the bimodal distribution of neutron-star masses, *The Astrophysical Journal* **719**, p. 722.
- Shao, D.-S., Tang, S.-P., Sheng, X., Jiang, J.-L., Wang, Y.-Z., Jin, Z.-P., Fan,

- Y.-Z., and Wei, D.-M. (2020). Estimating the maximum gravitational mass of nonrotating neutron stars from the gw170817/grb 170817a/at2017gfo observation, *Physical Review D* **101**, p. 063029.
- Shapiro, S. L. and Teukolsky, S. A. (2008). *Black holes, white dwarfs, and neutron stars: The physics of compact objects* (John Wiley & Sons, USA).
- Sharma, R. and Maharaj, S. (2007). A class of relativistic stars with a linear equation of state, *Monthly Notices of the Royal Astronomical Society* **375**, pp. 1265–1268.
- Sharma, S. (2017). Markov chain monte carlo methods for bayesian data analysis in astronomy, *Annual Review of Astronomy and Astrophysics* **55**, pp. 213–259.
- Shibata, M., Zhou, E., Kiuchi, K., and Fujibayashi, S. (2019). Constraint on the maximum mass of neutron stars using gw170817 event, *Physical Review D* **100**, p. 023015.
- Siess, L. (2007). Evolution of massive agb stars. ii. model properties at non-solar metallicity and the fate of super-agb stars, *Astronomy & Astrophysics* **473**, pp. 893–899.
- Stairs, I. H. (2003). Testing general relativity with pulsar timing, *Living Reviews in Relativity* **6**, p. 5.
- Steehgs, D. and Jonker, P. (2007). On the mass of the neutron star in v395 carinae/2s 0921–630, *The Astrophysical Journal Letters* **669**, p. L85.
- Stovall, K., Freire, P., Antoniadis, J., Bagchi, M., Deneva, J., Garver-Daniels, N., Martinez, J., McLaughlin, M., Arzoumanian, Z., Blumer, H., *et al.* (2019). Psr j2234+ 0611: a new laboratory for stellar evolution, *The Astrophysical Journal* **870**, p. 74.
- Sukhbold, T., Ertl, T., Woosley, S., Brown, J. M., and Janka, H.-T. (2016). Core-collapse supernovae from 9 to 120 solar masses based on neutrino-powered explosions, *The Astrophysical Journal* **821**, p. 38.
- Suwa, Y., Yoshida, T., Shibata, M., Umeda, H., and Takahashi, K. (2018). On the minimum mass of neutron stars, *Monthly Notices of the Royal Astronomical Society* **481**, pp. 3305–3312.
- Tauris, T., Kramer, M., Freire, P., Wex, N., Janka, H.-T., Langer, N., Podsiadlowski, P., Bozzo, E., Chaty, S., Kruckow, M., *et al.* (2017). Formation of double neutron star systems, *The Astrophysical Journal* **846**, p. 170.
- Tetarenko, B., Bahramian, A., Arnason, R., Miller-Jones, J., Repetto, S., Heinke, C., Maccarone, T., Chomiuk, L., Sivakoff, G., Strader, J., *et al.* (2016). The first low-mass black hole x-ray binary identified in quiescence outside of a globular cluster, *The Astrophysical Journal* **825**, p. 10.
- Thirukkanesh, S. and Ragel, F. (2012). Exact anisotropic sphere with polytropic equation of state, *Pramana* **78**, pp. 687–696.
- Thorsett, S. E. and Chakrabarty, D. (1999). Neutron star mass measurements. i. radio pulsars, *The Astrophysical Journal* **512**, p. 288.
- Tian, W. and Leahy, D. (2004). 20 pairs of real pulsar/supernova remnant associations, in *Symposium-International Astronomical Union*, Vol. 218 (Cambridge University Press, UK), pp. 137–138.
- Timmes, F., Woosley, S., and Weaver, T. A. (1996). The neutron star and black

- hole initial mass function, *The Astrophysical Journal* **457**, pp. 834–850.
- Tolman, R. (1934). Relativity, thermodynamics, and cosmology. clarendon, .
- Tomsick, J. A., Gelino, D. M., Halpern, J. P., and Kaaret, P. (2004). The low quiescent x-ray luminosity of the neutron star transient xte j2123–058, *The Astrophysical Journal* **610**, p. 933.
- Ugliano, M., Janka, H.-T., Marek, A., and Arcones, A. (2012). Progenitor-explosion connection and remnant birth masses for neutrino-driven supernovae of iron-core progenitors, *The Astrophysical Journal* **757**, p. 69.
- Umeda, H., Nomoto, K., Yamaoka, H., and Wanajo, S. (1999). Evolution of $3\text{-}9 m_{\odot}$ stars for $z=0.001\text{-}0.03$ and metallicity effects on type ia supernovae, *The Astrophysical Journal* **513**, pp. 861–868.
- Valentim, R., Rangel, E., and Horvath, J. (2011). On the mass distribution of neutron stars, *Monthly Notices of the Royal Astronomical Society* **414**, 2, pp. 1427–1431.
- van den Heuvel, E. (2004). X-ray binaries and their descendants: binary radio pulsars; evidence for three classes of neutron stars? *arXiv preprint astro-ph/0407451* .
- van den Heuvel, E. P. (2018). High-mass x-ray binaries: progenitors of double compact objects, *Proceedings of the International Astronomical Union* **14**, S346, pp. 1–13.
- Van Kerkwijk, M., Breton, R., and Kulkarni, S. (2011). Evidence for a massive neutron star from a radial-velocity study of the companion to the black-widow pulsar psr b1957+ 20, *The Astrophysical Journal* **728**, p. 95.
- Van Leeuwen, J., Kasian, L., Stairs, I. H., Lorimer, D., Camilo, F., Chatterjee, S., Cognard, I., Desvignes, G., Freire, P., Janssen, G., *et al.* (2015). The binary companion of young, relativistic pulsar j1906+ 0746, *The Astrophysical Journal* **798**, p. 118.
- Wang, B. and Liu, D. (2020). The formation of neutron star systems through accretion-induced collapse in white-dwarf binaries, *arXiv preprint arXiv:2005.01880* .
- Weber, F. (2017). *Pulsars as astrophysical laboratories for nuclear and particle physics* (Routledge, London).
- Weisberg, J. M., Nice, D. J., and Taylor, J. H. (2010). Timing measurements of the relativistic binary pulsar psr b1913+ 16, *The Astrophysical Journal* **722**, p. 1030.
- Witten, E. (1984). Cosmic separation of phases, *Physical Review D* **30**, p. 272.
- Woosley, S., Sukhbold, T., and Janka, H.-T. (2020). The birth function for black holes and neutron stars in close binaries, *The Astrophysical Journal* **896**, p. 56.
- Wu, X., Du, S., and Xu, R. (2020). What if the neutron star maximum mass is beyond $\sim 2.3m_{\odot}$? *Monthly Notices of the Royal Astronomical Society* .
- Zhang, C., Wang, J., Zhao, Y., Yin, H., Song, L., Menezes, D., Wickramasinghe, D., Ferrario, L., and Chardonnet, P. (2011). Study of measured pulsar masses and their possible conclusions, *Astronomy & Astrophysics* **527**, p. A83.
- Zhu, W., Stairs, I., Demorest, P. B., Nice, D. J., Ellis, J., Ransom, S., Arzou-

Bibliography

53

manian, Z., Crowter, K., Dolch, T., Ferdman, R., *et al.* (2015). Testing theories of gravitation using 21-year timing of pulsar binary j1713+ 0747, *The Astrophysical Journal* **809**, p. 41.